5-2011

Comparison of Baseflow-Stormflow Ion Mass Export for Two Streams in the Great Smoky Mountains National Park

Guy Thomas Zimmerman
gzimmer1@utk.edu

To the Graduate Council:

I am submitting herewith a thesis written by Guy Thomas Zimmerman entitled "Comparison of Baseflow-Stormflow Ion Mass Export for Two Streams in the Great Smoky Mountains National Park." I have examined the final electronic copy of this thesis for form and content and recommend that it be accepted in partial fulfillment of the requirements for the degree of Master of Science, with a major in Environmental Engineering.

John, S, Schwartz, Major Professor

We have read this thesis and recommend its acceptance:

R. Bruce Robinson, Glenn A. Tootle

Accepted for the Council:
Carolyn R. Hodges

Vice Provost and Dean of the Graduate School

(Original signatures are on file with official student records.)

Comparison of Baseflow-Stormflow Ion Mass Export for Two Streams in the Great Smoky Mountains National Park

A Thesis Presented for the
Master of Science
Degree
The University of Tennessee, Knoxville

Guy Thomas Zimmerman
May 2011

ACKNOWLEDGEMENTS

I would like to thank Dr. John Schwartz for providing me with this opportunity and for his patience and guidance throughout the course of this research. I would also like to thank the members of my committee, Dr. Bruce Robinson and Dr. Glenn Tootle. Several other students were vital in data collection and consultation including Dr. Keil Neff, Dr. Meijun Cai, Joseph Parker, Edwin Deyton, William Cantrell, and Lee Mauney. This research would not have been possible without Steve Moore and Matt Kulp of the Great Smoky Mountains National Park. My parents, Guy and Paula Zimmerman, deserve recognition for their support. Thanks to my wife, Sarah Zimmerman, for her patience, guidance, consultation, and partnership throughout this endeavor. Finally, I would like to acknowledge the beauty and magnificence of the streams of the Great Smoky Mountains.

ABSTRACT

This study characterizes the mass transport of ions in two streams in the Great Smoky Mountains National Park, comparing transport between stormflow and baseflow periods. By comparing ion mass transport between these two hydrological conditions, the importance of soil and the governing biogeochemical processes will be underscored. Two water quality monitoring study sites were located on the Middle Prong of the Little Pigeon River and Ramsey Prong within the same basin. These remote sites were equipped with YSI 6920 multi-parameter sonde to record continuous 15-min data of pH, depth, conductivity, turbidity, and temperature. Additionally, ISCO 6712 composite samplers were used to collect stream samples during storm events. Baseflow was collected by grab samples prior to storm events, and stormflow collected by ISCO samplers. Throughfall samples were collected after storm events. All samples were analyzed for pH, ANC, and conductivity using an autotitrator. Inductively coupled plasma spectrometry and ion chromatography were used to determine major cations, trace metals, and anions (Ca^{2+}, Na^{+}, K^{+}, Mg^{2+}, Al^{n+}, Cu, Fe, Mn, Si, Zn, SO_4^{2-}, NO_3^{-}, Cl^{-}, NH_4^{+}). Stage-discharge relationships were developed at each site utilizing a combination of field measurements and modeling. Velocity and area field measurements were taken to calculate discharges for mid- to low-flow stages while mid- to upper-flow stages were modeled using RIVER2D and verified with field measurements. Stage-discharge curves and sample ion concentrations were used to compute ion mass transport for a two year period in 2006 through 2008. Differences in mass transport of ions between baseflow and stormflow periods found that greater mass transport of ions, except protons, occurred

during baseflow periods. These results indicate that on an annual basis ions are stored from input throughfall sources and released gradually through groundwater flow over time more than rapid interflow transport during storm events. This information illustrates the importance of soils and groundwater storage in the regulation of ion transport and streamwater quality in the Great Smoky Mountains National Park.

TABLE OF CONTENTS

List of Tables

LIST OF FIGURES

CHAPTER I
INTRODUCTION AND GENERAL INFORMATION

Episodic acidification (EA) is a phenomenon affecting watersheds in northern Europe and eastern North America (Driscoll *et al.* 2001). Especially vulnerable are small high elevation watersheds with low acid neutralizing capacity (ANC) values that receive large amounts of atmospheric acidic deposition from anthropogenic pollutants such as sulfates and nitrates (Herlihy *et al.* 1993; Deviney *et al*. 2006). Numerous streams of the Appalachian Mountains have been recorded as being affected by EA, and the biogeochemical processes responsible for EA vary spatially and temporally (Herlihy *et al.* 1993). Due to the combination of its watershed setting and levels of acidic deposition, the Great Smoky Mountains National Park (GRSM) has several streams shown to experience EA (Shubdza *et al.* 1995; NADP 2007; Deyton *et al.* 2008; Cai et. 2009). EA has been demonstrated to cause significant sublethal physiological stress in native brook trout (*Salvelinus Fontinalis*) (Neff *et al.* 2009). Resource managers of the GRSM have expressed concern that EA may be a significant factor in the decline of native brook trout in some headwater steams in the GRSM (Deyton *et al.* 2008; Neff *et al*. 2009; Cai *et al.* 2010).

Episodic acidification is the short-term decrease in ANC, including to negative values, during high streamflow (Wigington *et al*. 1990; Wellington and Driscoll 2004). In the GRSM, natural processes responsible for EA include base cation dilution, nitrification, organic acid flushing, and weathering of sulfitic geology (Huckabee *et al.* 1975; Wigington *et al*. 1990; Kahl *et al*. 1992; Mitchell *et al*. 2001), while major

anthropogenic contributions to EA include atmospheric deposition of nitrogen and sulfates (Herlihy *et al*. 1993; Wigington *et al*. 1996b). Numerous processes causing EA may occur in a single watershed, and the dominant mechanism of EA in a watershed can vary with climate and hydrological events (Tranter *et al*. 1994; Deyton *et al*. 2008). These processes are affected by complex biogeochemical interactions including hydrological soil flowpath variability, vegetative consistency and successional stage, soil adsorption/desorption capacity, seasonality, and elapsed time between climatic events (Molot *et al*. 1989; Tranter *et al*. 1994; Cook *et al*. 1994; Lawrence 2002; Wellington and Driscoll 2004; Cai *et al*. 2010). This variability results in great difficulty in predicting the occurrence, severity, and duration of episodic events (Eshleman *et al*. 1992; Kahl *et al*. 1992).

Streams generally exhibit differing chemistries when comparing baseflow to stormflow, where baseflows tend to have higher values of pH and ANC values (Deyton *et al*. 2008). Subsurface flow during baseflow conditions are thought to be from deep soil flowpaths that have higher concentrations of exchangeable base cations due to longer residence times allowing for more chemical dissolution (Cook *et al*. 1994; Wagner *et al*. 2008). Storm events cause a shift in subsurface flow to shallow soil layers that contain greater concentrations of acidic ions from sulfate, nitrate, and organic anions (Kahl *et al*. 1992; Laudon *et al*. 2000). Storm events also transport anthropogenic acidic ions that have collected on vegetation from dry deposition, i.e. throughfall, into the stream during subsequent hydrological events. Finally, the acidic ions in precipitation also act to decrease stream ANC during stormflow.

Studies of the stream chemistry in the GRSM have shown EA can occur from changes to the stream chemistry caused by increased concentrations of nitrates and sulfates, base cation dilution, and organic acid flushing (Cook *et al*. 1994, Deyton *et al*. 2008; Cai *et al*. 2010). Research on the biogeochemical factors influencing long term EA at a high elevation site (Noland Divide) in the GRSM has shown net export of nitrates, sulfates, and exchangeable base cations, suggesting the predictability of future acidification events in GRSM streams may be strongly influenced by the ability of soil and plant vegetation to adsorb, retain, and release chemical ions important to stream chemistry (Cai *et al*. 2010, Cai in preparation). Despite efforts to decrease the amount of acidic pollutants in the atmosphere, numerous streams in the GRSM and other Appalachian Mountain regions have not shown significant recovery from acidification (Webb at al. 2004; Simonin *et al*. 2005; NADP 2007; Robinson *et al*. 2008).

The objectives of this study were: 1) to develop annual and seasonal estimates of ion mass export for two streams in the GRSM, and 2) to compare the transport regimes for different ions and watersheds between baseflow and stormflow periods and between the dormant and transpiring seasons. In addition for purposes of characterizing ion inputs to the watersheds, annual estimates of throughfall mass will be estimated. We hypothesize that seasonal, flow regime, and size differences in streams in the GRSM affect the mass export of important chemical constituents on stream chemistry. This information will help resource managers develop effective goals to augment brook trout restoration activities.

CHAPTER II
MATERIALS AND METHODS

Study Area

Water quality was monitored at two stream sites in the Middle Prong of the Little Pigeon (MPLP) River watershed in the GRSM (Figure 1). The MPLP watershed provides drainage for 117.4 km^2 within the GRSM boundary (Deyton *et al*. 2008). The climate of the GRSM is classified as perhumid mesothermal with variation of precipitation and seasonal temperature distributed throughout the year (Busing 2005). The average annual temperature at the Gatlinburg SW station between 1978 and 1992 was 13.2°C with a precipitation annual average of 141 cm (Busing 2005). The Alum Cave Bluffs Parking Area station is more representative of the MPLP watershed, and it had an annual average temperature of 9.9°C with an annual average precipitation of 200 cm from 1947-1950 (Shanks 1954).

The soils found in the watershed are typically thin, sandy loams. The geology tends to include base poor materials with sandstone, siltstone, shale, sand slate (King *et al*. 1968). Vegetation is generally thick with deciduous trees and increasing conifers with elevation. The MPLP is a steep watershed with an average slope of 25.4% (Deyton *et al*. 2008). The streams in the MPLP are typically dominated by boulder and cobble sized bed material with channel slopes between 5% and 12% (Larson *et al*. 1995). The streams in the MPLP generally have poor acidity buffering capability with acid neutralizing capacity (ANC) values including baseflow values below 50 (Neff *et al*. 2009).

Two study sites from the Deyton *et al*. (2008) and Neff *et al*. (2009) studies were selected for further analysis, the Middle Prong of the Little Pigeon River (MP1) and Ramsey Prong (MP2). Both sites were located to minimize anthropogenic effects on stream chemistry, and MP1 is accessible by 2.4 km of hiking trails from the nearest gravel road with MP2 located approximately an additional 1 km beyond MP1. The MP1 reach is approximately 150 m in length with an average channel slope of 4% and a drainage area of 38.7 km^2. MP1 is located just below the confluence of the Ramsey and Buck Prongs, and Eagle Rocks Prong, another major tributary that was researched in the previous studies, drains into the Buck Prong above the confluence with Ramsey Prong. MP1 is located in a fifth order mountain stream while MP2 is sited in a fourth order mountain stream. The MP2 reach is approximately 69 m in length with an average channel slope of 7.25% and draining 10.3 km^2.

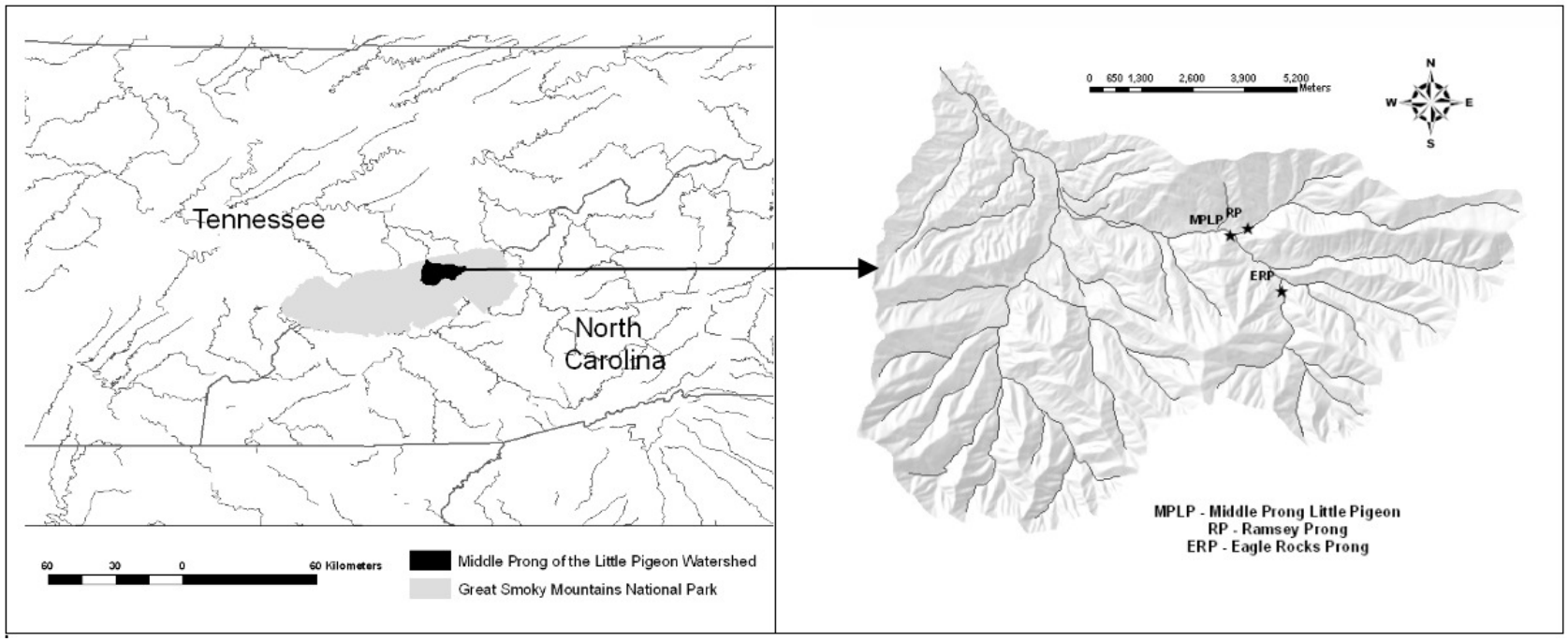

Figure 1. Location map from Neff *et al.* 2009. Used with permission. Please note Eagle Rocks Prong site not used in this study.

Study Design

Stream chemistry was analyzed at the two sites from February 2006 through February 2008. YSI 6920 multi-parameter sondes recorded temperature, specific conductance, stage, pH, and turbidity in 15-minute increments. The sites also had ISCO 6712 composite samplers that were programmed to collect water samples upon triggering from an incremental increase in stage or decrease in pH. The ISCO units collected samples every 45 minutes during the first six hours of a storm event. After six hours of the event had passed, samples were then collected every two hours for the next 30 hours. Grab samples were collected at least monthly and occasionally before storm events. Bulk throughfall precipitation samples were collected in eight inch plastic funnels that fed into plastic buckets. All samples were collected in LDPE bottles that were triple rinsed with deionized water in the lab. Grab and throughfall samples were additionally triple rinsed with sample water in the field prior to sampling.

Chemical analysis of the stream samples occurred in the Civil and Environmental Engineering Water Quality Laboratory at the University of Tennessee in Knoxville. Analyses included pH and ANC through titration and conductivity through a probe with a Mantech autotitrator, major cations (Ca, Na, K, Mg, Al, Cu, Fe, Mn, Si, and Zn) using a Thermo-Electron inductively-coupled plasma (ICP) spectrometer, and anions (nitrates, sulfates, and chloride) and ammonium using a Dionex ion chromatograph (IC). A laboratory QA/QC program was followed and is detailed in Cai (2010). The change in ANC calculation is detailed in Deyton *et al*. (2008), and it is based on the modified Molot *et al.* (1989) method as detailed in Hyer *et al*. (1995).

Stage-discharge relationships were developed through a combination of velocity-area measurements and hydraulic modeling. The velocity measurements were made with electromagnetic current meter (FLOWMATE2000™), and the velocity measurements were made using the Six-Tenths Depth Method as detailed in USGS Water-Supply Paper 2175 (Rantz *et al*. 1983). Due to the nature and location of the streams, gathering velocity measurements at stages near the maximum recorded stages would have been extremely difficult and potentially dangerous. As a result, the computer software River2D was utilized to model flows at both extremes of the stage-discharge curves.

River2D is a depth averaged, finite element model that utilizes conservation of mass and two horizontal components of conservation of momentum (Steffler and Blackburn 2002). Basic operation of the model requires topographic data imported to the model via a bed editing program. This information is then transferred to a mesh editing software that generates flow boundaries, no flow boundaries, and a triangular mesh connected via "floating nodes." The mesh is then imported into the River2D program, where calculations are made at the floating nodes and averaged across the individual triangles.

An extensive survey of the reaches surrounding the sondes at M1 and M2 provided the necessary topographic data for the computer model. The steepness and bedforms of the channel proved a difficult prospect for River2D, and successful models were obtained to effectively extend the stage-discharge relationships. The maximum and minimum field measured stage-discharge relations were modeled to calibrate the software. Success was determined if the following conditions were achieved:

1. Stability of the model was maintained through the entire run
2. Unrealistic and/or "spurious velocities" (Steffler and Blackburn 2002) and associated calculated values (i.e. Froude number) were minimized locally and in magnitude to not significantly affect inflow, outflow, or sonde area values of depth, velocity, and discharge
3. Inflow equaled outflow within 5%
4. Field measured stage-discharge values equaled modeled stage-discharge values within 5% for calibration model runs

The field equipment used in this experiment was deployed for two years in the some of the harshest environments found in the southeast United States. Flood events, wildlife, freezing temperatures, low conductivity streamwater, and curious hikers all caused equipment malfunctions where small sections of data were missing. If the sonde at one location malfunctioned, pH and depth measurements were estimated from depth and pH measurements at the other sonde through regression equations. No sonde data existed at either reach for ten days in May 2006 and forty-eight days in September and October 2007. The data for these sections was omitted, and any comparison of annual estimates was normalized for the number of days actually collected during the year

Hydrograph separation of stormflow and baseflow categories was accomplished through analysis of monthly discharge and pH plots. Episodes of acidification were identified and defined as a decrease in pH greater than 0.2 units with a measurable increase in flow. The end of the episode was arbitrarily defined as the time where the pH

curve shows a noticeable inflection point as the slope flattens during recovery. Figure 2 shows a typical response with delineation of baseflow and stormflow.

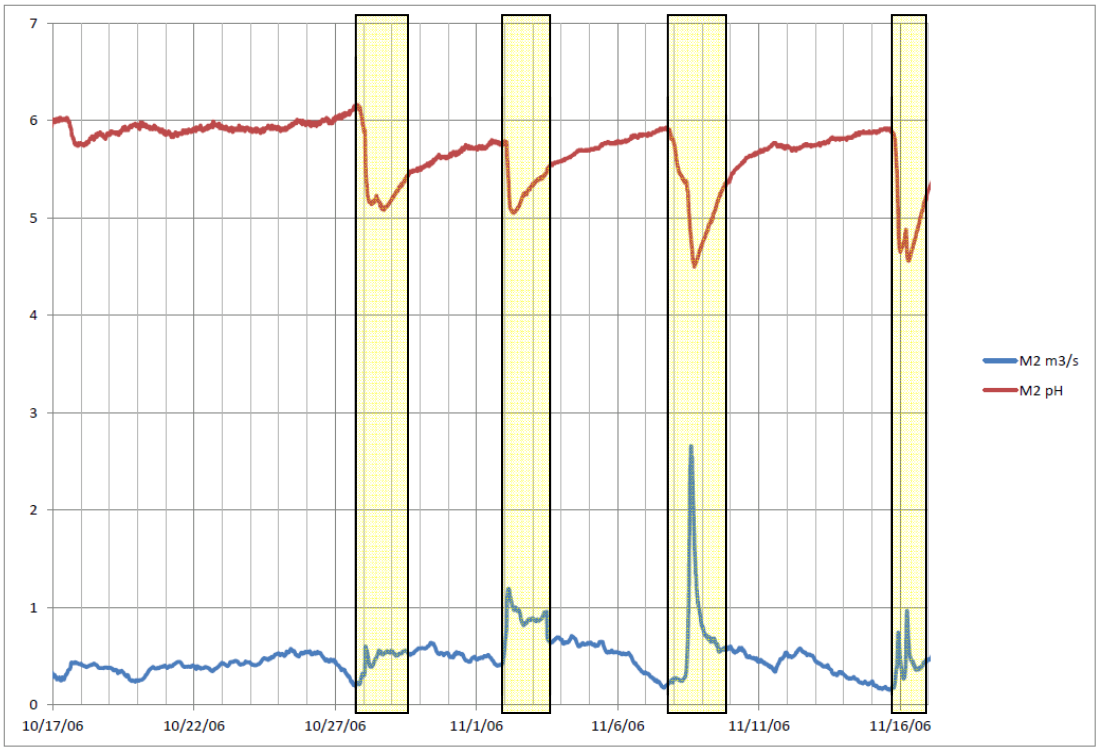

Figure 2. Typical pH-discharge response with delineation of Stormflow in yellow

Regression equations were developed to estimate mass in equivalents (eq) from discharge for the ions of Cl^-, NO_3^-, SO_4^{-2}, NH_4^+, Na^+, K^{+2},Mg^{+2}, and Ca^{+2}. All regression fittings and equations are provided as Appendix D. The mass estimate of H^+ came directly from the pH measurement. Throughfall mass loading rate estimates were calculated by averaging the concentration and multiplying by the average annual

precipitation for each ion. The mass in equivalents was estimated for every 15-minute increment of sonde data based on the discharge for time increment, and these mass estimates were coded in a database to differentiate base, storm, dormant, and transpiring periods. The mass for each ion was summed according to the analysis being conducted to achieve mass estimates of observed data. Conversion of these estimates to loading rates were normalized according to actual amount of time where data were successfully collected (i.e. 2006 has 351 successful days of collected data, therefore the 2006 annual estimates would multiply the mass by the ratio365/351). Also included in the conversion to loading rates was accounting for drainage area based on hectares, where MP1 drains 3,870 ha and MP2 drains 1,030 ha. The year 2006 is defined in this study as 2/17/2006 to 2/14/2007, and the year 2007 is defined as 2/15/2007 to 2/14/2008.

CHAPTER III

RESULTS

Stage-Discharge Relationships

Velocity and area measurements were obtained for flows ranging from 1.06 to 4.69 m^3/s at M1 and 0.28 to 3.57 m^3/s at M2. This corresponds to stage ranges from 0.70 to 0.98 m at M1 and 0.88 to 1.11 m at M2. However, recorded stage from at M1 ranged from 0.42 m to 1.62 m and M2 ranged from 0.57 m to 1.79 m. Modeled results extended the range at M1 to 0.50 through 1.55 m, and M2 range was extended to 0.59 through 1.87 m.

The results of the model were plotted, and the following regression equations were determined:

1. M1 discharge (m^3/s) = $5.859*(\text{M1 stage (m)})^{4.5128}$
2. M2 discharge (m^3/s) = $1.0482*(\text{M2 stage (m)})^{4.8137}$

Screenshots of the River2D results are included as Appendix B, and the stage-discharge plots are included as Appendix C.

Water Volume Estimates

The stage-discharge rating curves were used to estimate the amount of water volume that was transported in each 15-minute increment of the data set. Two hundred centimeters of annual precipitation was assumed in the calculation of stream export of water in the watersheds, and M1 had total stream export of 72.4%, 2006 stream export of 72.8%, and 2007 stream export of 72.2%. M2 experienced total stream export of water at

77.8%, 2006 stream export of 89.3%, and 2007 stream export 65.8%. Export is defined in this study as when a substance is transported beyond the boundary of the physical system being investigated via a stream. Inputs into the system can be exported out of the system, become losses such as evapotranspiration or groundwater leakage, or be retained indefinitely in the system in the soil or vegetation.

It is important to note that southeast U.S. experienced a major drought during the years of 2007 and 2008. It appears that M2 was affected to a greater degree than M1 by the drought, as M1 did not see much decline as a percentage of its total water budget between the years of 2006 to 2007.

After performing hydrograph separation for 60 hydrological storm events, estimates of water volume transported during storm, base, dormancy, and transpiration regimes and times were also determined. Table 1 details the water volume estimates, and Table 2 provides volume percentages for different flow conditions. Table 3 provides time details for stormflow and baseflow. Export is defined in this study as when a substance is transported beyond the boundary of the physical system being investigated via a stream. Inputs into the system can be exported out of the system, become losses such as evapotranspiration or groundwater leakage, or be retained in the system in the soil or vegetation.

Table 1. Streamflow, stormflow, baseflow, transpiration and dormant volumes

Site	M1	M2
Total Streamflow Volume (m^3)	112,126,810	32,062,732
Total Stormflow Volume (m^3)	28,490,426	6,382,187
Total Baseflow Volume (m^3)	83,636,384	25,680,545
2006 Streamflow Volume (m^3)	56,383,290	18,392,941
2006 Stormflow Volume (m^3)	15,850,432	4,287,879
2006 Baseflow Volume (m^3)	40,532,858	14,105,062
2007 Streamflow Volume (m^3)	55,892,014	13,553,069
2007 Stormflow Volume (m^3)	12,570,864	2,027,128
2007 Baseflow Volume (m^3)	43,321,151	11,525,941
Total Transpiration Volume (m^3)	51,717,319	16,179,098
Total Dormant Volume (m^3)	60,379,491	15,883,634

Table 2. Stormflow and baseflow volume percentages for M1 and M2

Site	M1	M2
Total Stormflow Volume (%)	25%	20%
Total Baseflow Volume (%)	75%	80%
2006 Stormflow Volume (%)	28%	23%
2006 Baseflow Volume (%)	72%	77%
2007 Stormflow Volume (%)	22%	15%
2007 Baseflow Volume (%)	78%	85%

Table 3. Stormflow and baseflow time percentages for M1 and M2

Site	M1		M2	
	Days	%	Days	%
Total Time Stormflow	87.3	13%	88.6	13%
Total Time Baseflow	592.8	87%	591.5	87%
2006 Time Stormflow	53.5	15%	54.7	16%
2006 Time Baseflow	297.8	85%	296.6	84%
2007 Time Stormflow	33.8	10%	33.8	10%
2007 Time Baseflow	294.9	90%	294.9	90%

Mass Estimates

Throughfall

The throughfall data set for both sites is displayed in Table 4. The data collection for throughfall experienced multiple interferences from wildlife throughout the course of the project. Bears often destroyed throughfall equipment. As a result, often the volume of water in the throughfall buckets had to be assumed based on the other site's volume, and the volumes tended to be equivalent, especially during the fall and winter, due to the proximity between the two sites. This data is presented here to aid in the characterization of the ion input. Due to the paucity of throughfall samples (M1 = 24 and M2 =22) coupled with the large variability exhibited by the samples, caution should be exercised when applying estimates of mass loadings and comparisons for retained/export in the system.

Table 4. Throughfall average concentrations, standard deviations, mass, and mass loadings for M1 and M2 for 5/31/2006 to 2/14/2008

Ion	M1				M2			
	Average Conc. (µeq/l)	Std. Dev. (µeq/l)	Mass (eq)	Mass (eq/ha /yr)	Average Conc. (µeq/l)	Std. Dev. (µeq/l)	Mass (eq)	Mass (eq/ha/ yr)
Cl^-	12.71	9.95	1,683,944	256	17.05	15.39	600,284	343
NO_3^-	15.81	13.16	2,095,244	319	13.76	13.87	484,538	277
SO_4^{2-}	40.80	17.65	5,407,990	823	56.09	29.53	1,975,451	1129
NH_4^+	13.90	21.19	1,841,939	280	8.29	7.19	291,866	167
H^+	5.36	11.04	710,989	108	6.20	10.71	218,416	125
Na^+	10.35	9.71	1,371,280	209	14.70	15.07	517,854	296
K^+	37.70	44.62	4,996,521	760	47.81	26.25	1,683,807	962
Mg^{2+}	22.04	23.56	2,920,713	444	29.12	20.78	1,025,436	586
Ca^{2+}	55.93	37.91	7,412,371	1128	54.48	40.69	1,918,676	1097

Streamflow

Tables 5 and 6 detail the estimated mass for each ion for sites M1 and M2, respectively. Most ions have similar levels of mass loading in comparing site M1 against M2, with the exceptions of nitrates, sulfates, and sodium. Surprisingly, M1 appears to be exporting more sulfate than M2 despite an apparent greater deposition rate at the higher elevation of M2. This may be due to drought effects, as M1 and M2 transported similar totals of sulfate in 2006, but in 2007 M2's water transport was more affected than M1.

In comparison of the mass loading rates between 2006 and 2007, it is evident that the drought year of 2007 affected site M2's overall ability to transport mass to a greater degree than M1. This observation was also made from total streamflow volumes. The drought also caused M1 to transport approximately 5% more mass during baseflow in 2007 as compared to 2006, while M2 transported approximately 8% more mass during baseflow in 2007 as compared to 2006.

While some ions exhibited marginal, if any, differences in seasonality transport, site M2 had approximately 62% of nitrate transported during the dormant period.

At both sites mass export of all solutes is dominated by baseflow, except the case of H^+. More proton mass was transported during stormflow in 2006, but 2007 saw a reversal of that trend at M2 and M1 was nearly equivalent.

Table 5. Site M1 Ion Mass Summary in eq for Total Streamflow, Stormflow, Baseflow, Dormant, and Transpiration

Category	Estimated Cl^-	Estimated NO_3^-	Estimated SO_4^{2-}	Estimated NH_4^+	Measured; Estimated H^+	Estimated Na^+	Estimated K^+	Estimated Mg^{2+}	Estimated Ca^{2+}
Total eq	1,216,776	3,834,004	5,573,434	121,993	392,647	2,485,912	1,326,611	2,792,843	5,726,663
Total Storm eq	306,925	1,134,270	1,421,333	39,961	227,237	630,030	322,568	760,946	1,576,363
Total Base Eq	909,851	2,699,735	4,152,101	82,032	165,410	1,855,881	1,004,044	2,031,897	4,150,300
2006 eq	633,028	1,940,195	2,899,857	63,631	209,379	1,293,349	689,954	1,453,987	2,981,655
2006 Storm eq	173,709	609,642	803,800	22,245	132,303	356,455	183,050	428,385	886,834
2006 Base eq	459,319	1,330,554	2,096,057	41,386	77,077	936,894	506,904	1,025,602	2,094,821
2007 eq	583,748	1,893,809	2,673,577	58,362	183,268	1,192,563	636,657	1,338,856	2,745,008
2007 Storm eq	128,246	503,374	594,493	17,053	92,931	263,369	134,315	320,143	663,779
2007 Base eq	455,502	1,390,435	2,079,085	41,308	90,337	929,194	502,342	1,018,713	2,081,229
Total Dormant eq	654,557	1,960,739	2,999,624	66,476	183,168	1,337,555	712,525	1,507,620	3,092,828
Total Transpiration eq	562,219	1,873,265	2,573,810	55,517	209,479	1,148,357	614,086	1,285,223	2,633,836

Table 6. Site M2 Ion Mass Summary in eq Total Streamflow, Stormflow, Baseflow, Dormant, and Transpiration

Category	Estimated Cl^-	Estimated NO_3^-	Estimated SO_4^{2-}	Estimated NH_4^+	Measured; Estimated H^+	Estimated Na^+	Estimated K^+	Estimated Mg^{2+}	Estimated Ca^{2+}
Total eq	364,188	1,208,412	1,341,315	50,984	125,006	799,892	380,844	629,308	1,493,076
Total Storm eq	63,873	242,214	263,478	5,407	69,686	150,420	76,319	128,794	311,195
Total Base Eq	300,315	966,197	1,077,837	45,577	55,320	649,472	304,525	503,472	1,181,880
2006 eq	206,525	702,268	791,297	25,073	74,609	464,607	226,314	377,350	900,273
2006 Storm eq	42,070	157,950	177,999	3,003	45,927	100,674	51,772	87,659	212,762
2006 Base eq	164,455	544,317	613,297	22,071	28,682	363,933	174,542	290,333	687,510
2007 eq	157,663	506,144	550,019	25,911	50,397	335,284	154,530	251,957	592,803
2007 Storm eq	20,558	78,611	79,940	2,349	22,834	46,669	22,923	38,370	91,664
2007 Base eq	137,105	427,533	470,079	23,562	27,562	288,616	131,607	215,905	501,139
Total Dormant eq	184,327	744,003	666,072	27,409	51,001	400,253	188,435	311,886	733,309
Total Transpiration eq	179,861	464,409	675,243	23,576	74,005	399,638	192,409	317,422	759,767

Table 7. Site M1 Mass Transport in eq/ha for Total Streamflow, Stormflow, Baseflow, Dormant, and Transpiration

Category	Estimated Cl^-	Estimated NO_3^-	Estimated SO_4^{2-}	Estimated NH_4^+	Measured; Estimated H^+	Estimated Na^+	Estimated K^+	Estimated Mg^{2+}	Estimated Ca^{2+}
Total eq/ha	338	1,064	1,546	34	109	690	368	775	1,589
Total Storm eq/ha	85	315	394	11	63	175	89	211	437
Total Base eq/ha	252	749	1,152	23	46	515	279	564	1,151
2006 eq/ha	170	521	779	17	56	348	185	391	801
2006 Storm eq/ha	47	164	216	6	36	96	49	115	238
2006 Base eq/ha	123	358	563	11	21	252	136	276	563
2007 eq/ha	168	545	769	17	53	343	183	385	789
2007 Storm eq/ha	37	145	171	5	27	76	39	92	191
2007 Base eq/ha	131	400	598	12	26	267	144	293	598
Total Dormant eq/ha	182	544	832	18	51	371	198	418	858
Total Transpiration eq/ha	156	520	714	15	58	319	170	357	731

Table 8. Site M2 Mass Transport in eq/ha for Total Streamflow, Stormflow, Baseflow, Dormant, and Transpiration

Category	Estimated Cl^-	Estimated NO_3^-	Estimated SO_4^{2-}	Estimated NH_4^+	Measured; Estimated H^+	Estimated Na^+	Estimated K^+	Estimated Mg^{2+}	Estimated Ca^{2+}
Total eq/ha	380	1,259	1,398	53	130	834	397	656	1,556
Total Storm eq/ha	67	252	275	6	73	157	80	134	324
Total Base eq/ha	313	1,007	1,123	48	58	677	317	525	1,232
2006 eq/ha	209	709	799	25	75	469	228	381	909
2006 Storm eq/ha	42	159	180	3	46	102	52	89	215
2006 Base eq/ha	166	550	619	22	29	367	176	293	694
2007 eq/ha	170	547	594	28	54	362	167	272	640
2007 Storm eq/ha	22	85	86	3	25	50	25	41	99
2007 Base eq/ha	148	462	508	25	30	312	142	233	541
Total Dormant eq/ha	192	775	694	29	53	417	196	325	764
Total Transpiration eq/ha	187	484	704	25	77	417	201	331	792

Export

Comparison of the ion inputs to the stream export show that most ions are being retained to varying degrees in the system with the exceptions of nitrate and sodium. Table 9 details retention rates for all ions.

Table 9. Mass Retention Percentages

	M1			M2		
	Average Annual Input (eq/ha/yr)	**Average Annual Export (eq/ha/yr)**	**% Retained**	**Average Annual Input (eq/ha/yr)**	**Average Annual Export (eq/ha/yr)**	**% Retained**
Cl^-	256	169	34%	343	190	45%
NO_3^-	319	532	-67%	277	630	-127%
SO_4^{2-}	823	773	6%	1129	699	38%
NH_4^+	280	17	94%	167	27	84%
Total N	599	549	8%	444	657	-48%
H^+	108	54	50%	125	65	48%
Na^+	209	345	-65%	296	417	-41%
K^+	760	184	76%	962	198	79%
Mg^{+2}	444	387	13%	586	328	44%
Ca^{+2}	1128	794	30%	1097	778	29%

Depletion of sodium appears to be occurring at both sites, but other base cations appear to be retained. Depletion of base cations is a concern in regards to acidification because base cations help to moderate acidification. If more cations are depleted than enter the system, as some point the lack of exchangeable cations may allow for acidification to become more extreme and/or more chronic. While other research in the GRSM has shown a net depletion of calcium, magnesium, and sodium (Cai 2010), it appears that these sites are only experiencing sodium depletion.

Nitrate export may be overestimated due to nitrification of ammonia and nitrites. Ammonia is deposited and retained at much larger rates than any other ion, so it appears nitrogen cycling is active at these sites. Nitrification may be affecting the export of nitrate. The total nitrogen retention values in Table 9 show that nitrogen to may be retained at a very low rate at M1, while M2 still appears to be exporting nitrate after attempted correction to account for nitrification.

CHAPTER IV
DISCUSSION

The streams of the Great Smoky Mountains are unique in topography, geology, hydrology, and vegetation (Neff 2010). When comparing a GRSM mountain stream to a stream of comparable size at a lower elevation, there are several differences that affect the streams response to a hydrological event. Other researchers have found large variability on stream response when comparing similar basins of forested high elevation streams in the southern Appalachian mountains (Post and Jones 2001).

The steep topography transports water much faster giving the stream a quicker response to a storm event (Post and Jones 2001). Additionally, thin soils with high hydraulic conductivity provide faster hydrologic responses that over briefer time periods (Post and Jones 2001). Finally, the GRSM receives large amounts of precipitation due to orographic rain events, which often obfuscates identification of a well defined beginning and end to a hydrological event due to small, frequent rain events that overlap. In general, hydrograph separation is often an arbitrary and subjective exercise (Sloto and Crouse 1996).

These factors combine to make baseflow separation a difficult task. Analysis of the discharge and pH plots showed that both streams had varied pH responses to changes in discharges from hydrological events as seen in Figure 2. Often the pH response is a faster process than stormflow recession. In efforts to partition the categorical flows to examine the most negative flows, stormflow regimes in the traditional sense may have been shortened causing an over-representation of baseflow. If present, this over-

representation is largely the result of the arbitrary determination of where stormflow ends in the hydrograph. This may explain why baseflow so clearly dominated most mass export when other researchers have found stormflow to dominate in the GRSM (Cai 2010).

While a variety of methods exist for baseflow separation, it is not readily apparent from the literature which method may be most appropriate in the GRSM, and more study is needed to better describe the hydrological pathways, particularly related to inflow rates, within watersheds in the GRSM. These hydrological pathways are dependent on watershed characteristics, which have been shown to influence the acidification response (Kirchner *et al.* 1993).

Previous research at these sites showed evidence of variability in the acidification mechanisms at M1 (Deyton *et al.* 2008). Other researchers have shown that small, high elevation watersheds are more susceptible to episodic acidification (Deviney *et al.* 2006). Results from this study provide further documentation that stream size affects the response to episodic acidification. The smaller stream, M2, showed more susceptibility to seasonal influences in nitrate export, and it also demonstrated a larger effect from drought conditions on mass export. Several researchers have shown that drought conditions affect the magnitude and duration of EA (Laudon *et al.* 2004; Inamder *et al*. 2006; Deyton *et al.* 2008).

While the size of the stream may not control the quality and quantity of groundwater connections, generally the larger the stream, the further down it lies in the dendritic pattern of Appalachian streams. This would provide more chance for collection

of tributaries that may have better neutralization capabilities. Additionally, as the position in the dendritic pattern generally moves to lower elevations and higher stream orders, the geomorphology of the streams also change which allow for more retention over longer time periods of water (Post and Jones 2001).

Additional comparisons can be drawn from the smaller, high elevation GRSM streams at Noland Divide. At the NDW streams, mass transport tends to be dominated by stormflow (Cai 2010). NDW sees much higher rates of deposition from cloud deposition, conifer sweeping, and more orographic rain. NDW streams also transport more acidic ions per hectare, and they are currently exporting base cations. These streams appear to behave very differently, yet both areas experience the same phenomenon. Further qualification and quantification of this difference in behavior could prove useful for predicting future recovery as air quality and the climate change.

The relationship between pH and resulting mass is inversely logarithmic. While the other solutes regularly increase between on average 2 and 10 times in mass, hydrogen ions increase regularly by 100 times the pre-event mass during storm flows with the most extreme events increasing hydrogen mass by well over 1000 times the pre-event mass. The shear proportional differences between the equivalent mass at the extremes of the range of pH values experienced at these sites lends for proton to be dominated by stormflow. However, as baseflow pH drops to the low 5 range and remains for a moderate length of time, or in the prolonged absence of stormflow, it becomes more plausible that baseflow may be able to dominate proton transport at the year scale.

CHAPTER V
CONCLUSIONS

The Middle Prong of the Little Pigeon and its tributary the Ramsey Prong experience episodic acidification that is harmful to aquatic life (Neff *et al.* 2009). More than one process is occurring at the Middle Prong (Deyton *et al.* 2008), and the smaller, higher tributary of Ramsey Prong appears to be more susceptible to changes in stream chemistry and mass transport caused by drought conditions than the Middle Prong.

Nitrate and sodium are being exported from both sites, and nitrate export appears to be affected by seasonality. Contrary to research from the Noland Divide Watershed, mass export at the Middle Prong and Ramsey Prong were dominated by baseflow instead of stormflow. Hydrogen ions are the exception, and stormflow is expected to dominate mass transport of proton in all but the driest of years.

The current knowledge of hydrograph components for GRSM streams is lacking, and further research may benefit our understanding of base- and stormflow hydrological responses and processes. Expanding the knowledge base will allow for a better understanding of the watersheds response to a hydrological event.

REFERENCES

Busing, RT (2005) NPP Temperate Forest: Great Smoky Mountains, Tennessee, USA, 1978-1992. Data set. http://www.daac.ornl.gov Oak Ridge National Laboratory Distributed Active Archive Center.

Cai M, Schwartz JS, Robinson RB, Moore SE, Kulp, MA (2009) Long-Term Effects of Acidic Deposition on Water Quality in a High-Elevation Great Smoky Mountains National Park Watershed: Use of an Ion Input-Output Budget. Water Air and Soil Pollution **209:**143-156.

Cai M (2010) Long-term Acid Deposition Effects on Soil and Water Chemistry in the Noland Divide Watershed, Great Smoky Mountains National Park, USA. PhD dissertation, University of Tennessee.

Cook RB, Elwood JW, Turner RR, Bogle MA, Mullholland PJ, Palumbo AV (1994) Acid-base chemistry of high-elevation streams in the Great Smoky Mountain Mountains. Water Air and Soil Pollution **72:**331-356.

Deviney FA, Rice KC, Hornberger GM (2006) Time Series and recurrence interval models to predict the vulnerability of streams to episodic acidification in Shenandoah National Park, Virginia. Water Resources Research **42**.

Deyton EB, Schwartz JS, Robinson RB, Neff KJ, Moore SE, Kulp MA (2008) Characterizing episodic stream acidity during stormflows in the Great Smoky Mountain National Park. Water Air and Soil Pollution **196:**3-18.

Driscoll CT, Lawrence GB, Bulger AJ, Butler TJ, Cronan CS, Eager C, Lambert KF, Likens GE, Stoddard JL, Weathers KC (2001) Acidic Deposition in the Northeastern United States: Sources and Inputs, Ecosystem Effects, and Management Strategies. BioScience **51(3):**180-198.

Eshleman KN, Wigington PJ, Davies TD, Tranter M (1992) Modeling episodic acidification of waters: The state of science. Environmental Pollution **77:**287-295.

Herlihy AT, Kaufman PR, Church MR, Wigington PJ, Webb JR, Sale MJ (1993) The effects of acidic deposition on streams in the Appalachian Mountain and Piedmont Region of the Mid-Atlantic United States. Water Resources Research **29:**2687-2703.

Hewlett JD, Hibbert AR (1967) Factors affecting the response of small watersheds to precipitation in humid areas. International Symposium on Forest Hydrology 267-290.

Huckabee JW, Goodyear CP, Jones RD (1975) Acid Rock in the Great Smokies – Unanticipated Impact on Aquatic Biota of Road Construction in Regions of

Sulfide Mineralization. Transactions of the American Fisheries Society **104:**677-684.

Hyer KE, Webb JR, Eshleman KN (1995) Episodic acidification of three streams in Shenandoah National Park, Virginia, USA. Water Air and Soil Pollution **85:**523-528.

Kahl JS, Norton SA, Haines TA, Rochette EA, Heath RH, Nodvin SC (1992) Mechanisms of episodic acidification in low-order streams in Maine, USA. Environmental Pollution **78:**37-44.

Kirchner JW, Dillon PJ, LaZerte BD (1993) Separating Hydrological Geochemical Influences on Runoff Acidification in Spatially Heterogeneous Catchments. Water Resources Research **29(12):**3903-3916.

Inamdar SP, O'Leary N, Mitchell MJ, Riley JT (2006) The impact of storm events on solute exports from a glaciated forested watershed in western New York, USA. Hydrological Processes **20:**3423-3439.

King PB, Newman RB, Hadley JB (1968) Geology of the Great Smoky Mountains National Park, Tennessee and North Carolina. Professional Paper 587, United States Geologic Survey.

Larson GL, Moore SE, Carter B (1995) Ebb and flow of encroachment by nonnative rainbow trout in a small stream in the southern Appalachian Mountains. Transactions of the American Fisheries Society **114:**195-203.

Laudon H, Westling O, Bishop K (2000) Cause of pH decline in stream water during spring melt runoff in northern Sweden. Canadian Journal of Fisheries and Aquatic Sciences **57:**1888-1900.

Laudon H, Dillon PJ, Eimers MC, Semkin RG, Jeffries DS (2004) Climate-Induced Episodic Acidification of Streams in Central Ontario. Environmental Science and Technology **38:**6009-6015.

Lawrence GB (2002) Persistent episodic acidification of streams linked to acid rain effects on soil. Atmospheric Environment **36:**1589-1598.

Mitchell MJ, Mayer B, Bailey SW, Hornbeck JW, Alewell C, Driscoll CT, Likens GE (2001) Use stable isotopes ratios for evaluating sulfur sources and losses at the Hubbard Brook experimental forest. Water Air and Soil Pollution **130:**75-86.

Molot LA, Dillon PJ, LaZerte BD (1989) Factors Affecting Alkalinity Concentrations of Streamwater during Snowmelt in Central Ontario. Canadian Journal of Fisheries and Aquatic Sciences **46:**1658-1666.

National Atmospheric Deposition Program (2007) National Atmospheric Deposition Program 2006 Annual Summary. NADP Data Report 2007-01. Illinois State Water Survey, Champaign, IL.

Neff KJ, Schwartz JS, Henry TB, Robinson RB, Moore SE, Kulp MA (2009) Physiological Stress in Native Southern Brook Trout During Episodic Stream Acidification in the Great Smoky Mountain National Park. Archives of Environmental Contamination and Toxicology **57:**366-376.

Neff KJ (2010) Environmental Impacts to Stream Acidification and Brook Trout Populations in the Great Smoky Mountains National Park. PhD dissertation, University of Tennessee.

Post DA, Jones JA (2001) Hydrologic regimes of forested, mountainous, headwater basins in New Hampshire, North Carolina, Oregon, and Puerto Rico. Advances in Water Resources **24:**1195-1210.

Rantz SE *et al*. (1983) Measurement and Computation of Streamflow. Water-Supply Paper 2175 United States Geological Survey.

Robinson RB, Barnett TW, Harwell GR, Moore SE, Kulp MA, Schwartz JS (2008) pH and Acid Anion Time Trends in Different Elevation Ranges in the Great Smoky Mountains National Park. ASCE Journal of Environmental Engineering **134:**800-800.

Shanks RE (1954) Climates of the Great Smoky Mountains. Ecology **35:**354-361.

Shubzda J, Lindberg SE, Garten CT, Nodvin SC (1995) Elevational trends in the fluxes of sulphur and nitrogen in throughfall in the Southern Appalachian Mountains: Some surprising results. Water Air and Soil Pollution **85:**2265-2270.

Simonin HA, Colquhoun JR, Paul EA, Symula J, Dean HJ (2005) Have Adirondack Stream Fish populations Changed in Response to Decreases in Sulfate Deposition? Transactions of the American Fisheries Society **134:**338-345.

Sloto AS, Crouse YC (1996) HYSEP: A Computer Program for Streamflow Hydrograph Separation and Analysis. USGS Water-Resources Investigations Report 96-4040.

Steffler P, Blackburn J (2002) River2D User Manual.

Tranter M, Davies TD, Wigington PJ, Eshleman KN (1994) Episodic acidification of fresh-water systems in Canada – Physical and geochemical processes. Water Air and Soil Pollution **72:**19-39.

Wagner LE, Vidon P, Tedesco LP, Gray M. Stream nitrate and DOC dynamics during three spring storms across land uses in glaciated landscapes of the Midwest. Journal of Hydrology **362:**177-190.

Webb JR, Cosby BJ, Deviney FA, Galloway JN, Maben SW, Bulger AJ (2004) Are Brook Trout Streams in Western Virginia and Shenandoah National Park Recovering from Acidification? Environmental Science and Technology **38:**4091-4096.

Wellington BI, Driscoll CT (2004) The episodic acidification of a stream with elevated concentrations of dissolved organic carbon. Hydrological Processes **18:**2663-2680.

Wigington PJ, Davies TD, Tranter M, Eshleman KN (1990) Episodic acidification of surface waters due to acidic deposition. Acidic Deposition: State of Science and Technology, NAPAP Rep.12:200.

Wigington PJ, DeWalle DR, Murdoch PS, Kretser WA, Simonin HA, Vansickle J, Baker JP (1996b) Episodic acidification of small streams in the northeastern United States: Ionic controls of episodes. Ecological Applications **6:**389-407.

APPENDICES

Appendix A: Data Review and Validation

The data set used in this study came from field efforts undertaken in support of Master Theses for Edwin Deyton and Keil Neff during 2006, 2007, and 2008. Several people were involved in intensive data collection. During this time, the equipment deployed to the study sites malfunctioned at times. Despite corrective actions, including regular calibrations, replacement or repair of equipment, and field and lab measurements, there existed gaps in the 15 minute sonde data of completely missing or questionable data. In order to ameliorate the affects of missing and questionable data, the author performed an exhaustive review of stage and pH data.

Typical changes included estimating stage or pH data from surrounding linearly preceding and following data points and performing regressions to estimate stage or pH from the other study site's data. Total loss of sonde data was experienced at both sites at two separate occasions, May 5, 2006 to May 15, 2006 and September 7, 2007 to October 14, 2007. These times have been removed to normalize annual estimates provided previously.

Appendix B: River2D Model Result Screenshots

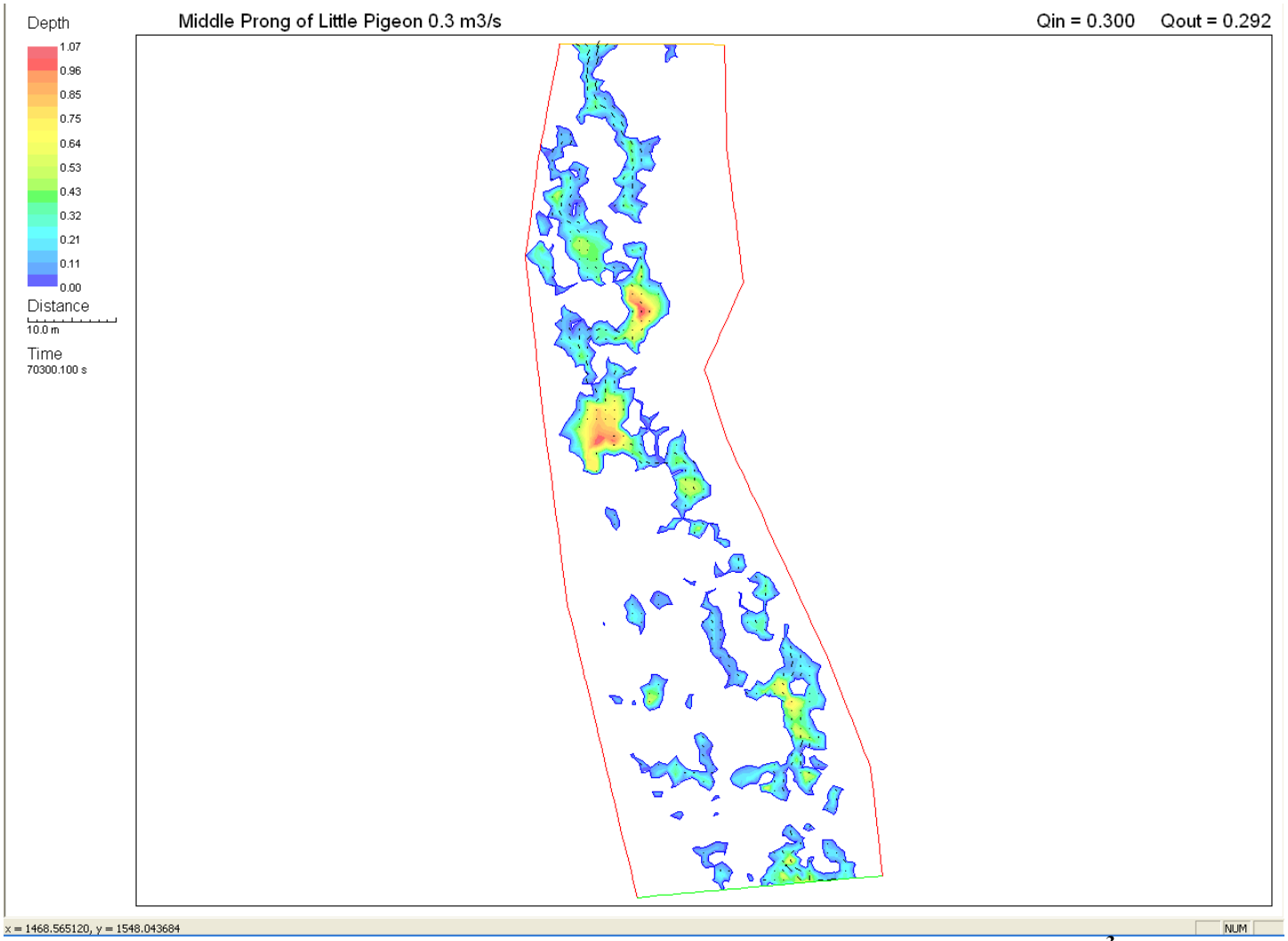

Figure 3. River2D results for depth at Middle Prong site for discharge of 0.3 m^3/s

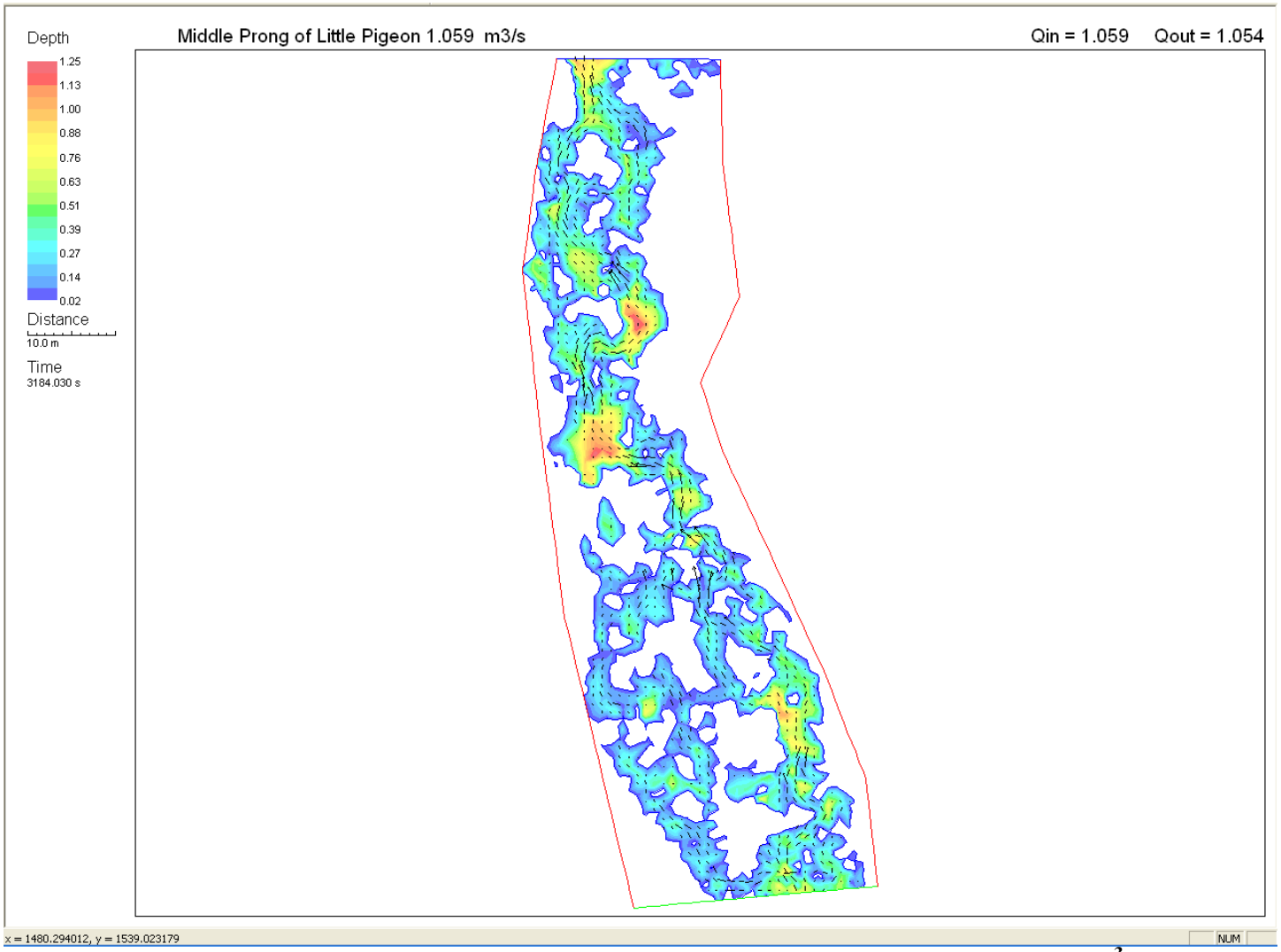

Figure 4. River2D results for depth at Middle Prong site for discharge of 1.059 m^3/s

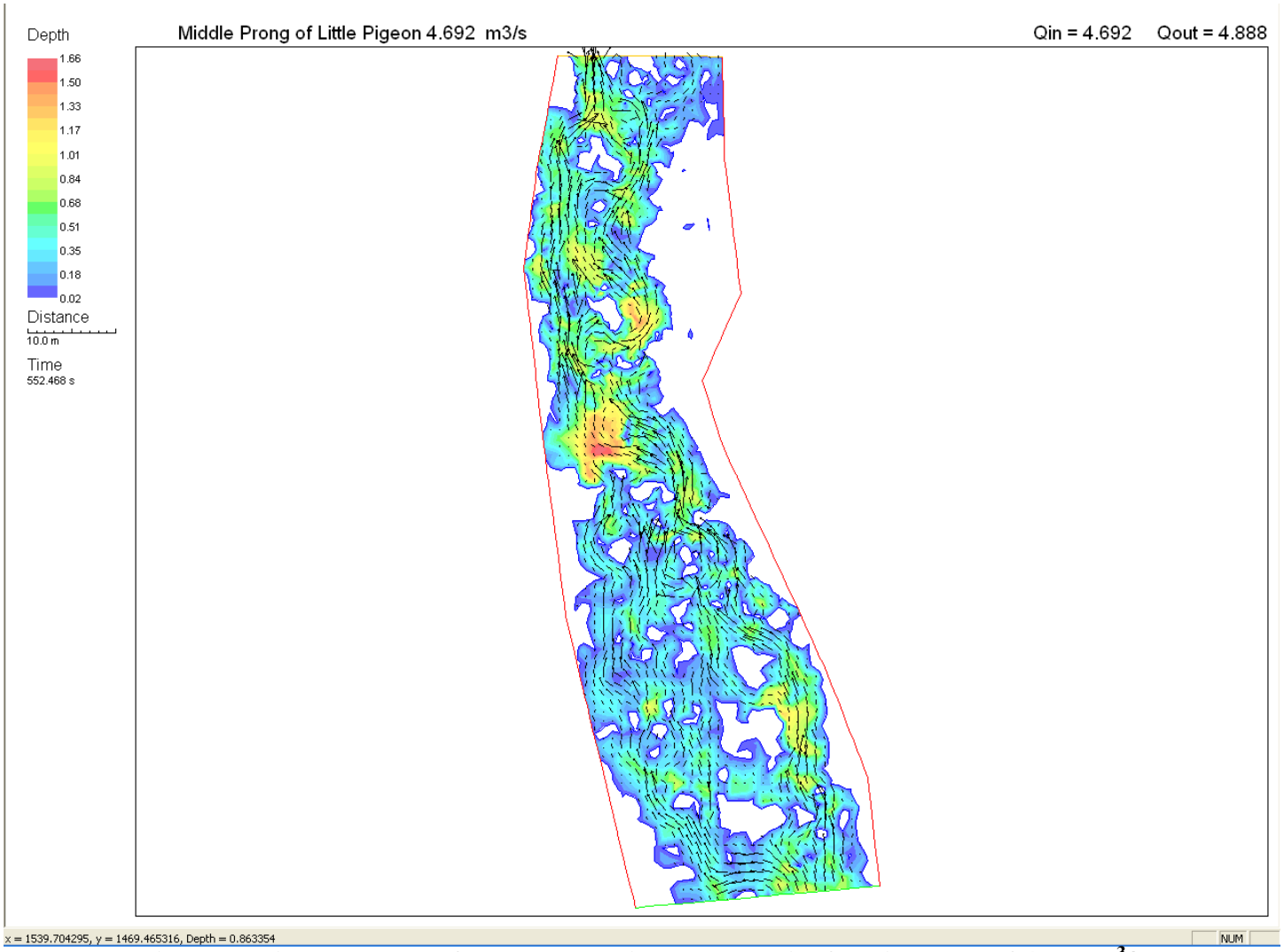

Figure 5. River2D results for depth at Middle Prong site for discharge of 4.692 m^3/s

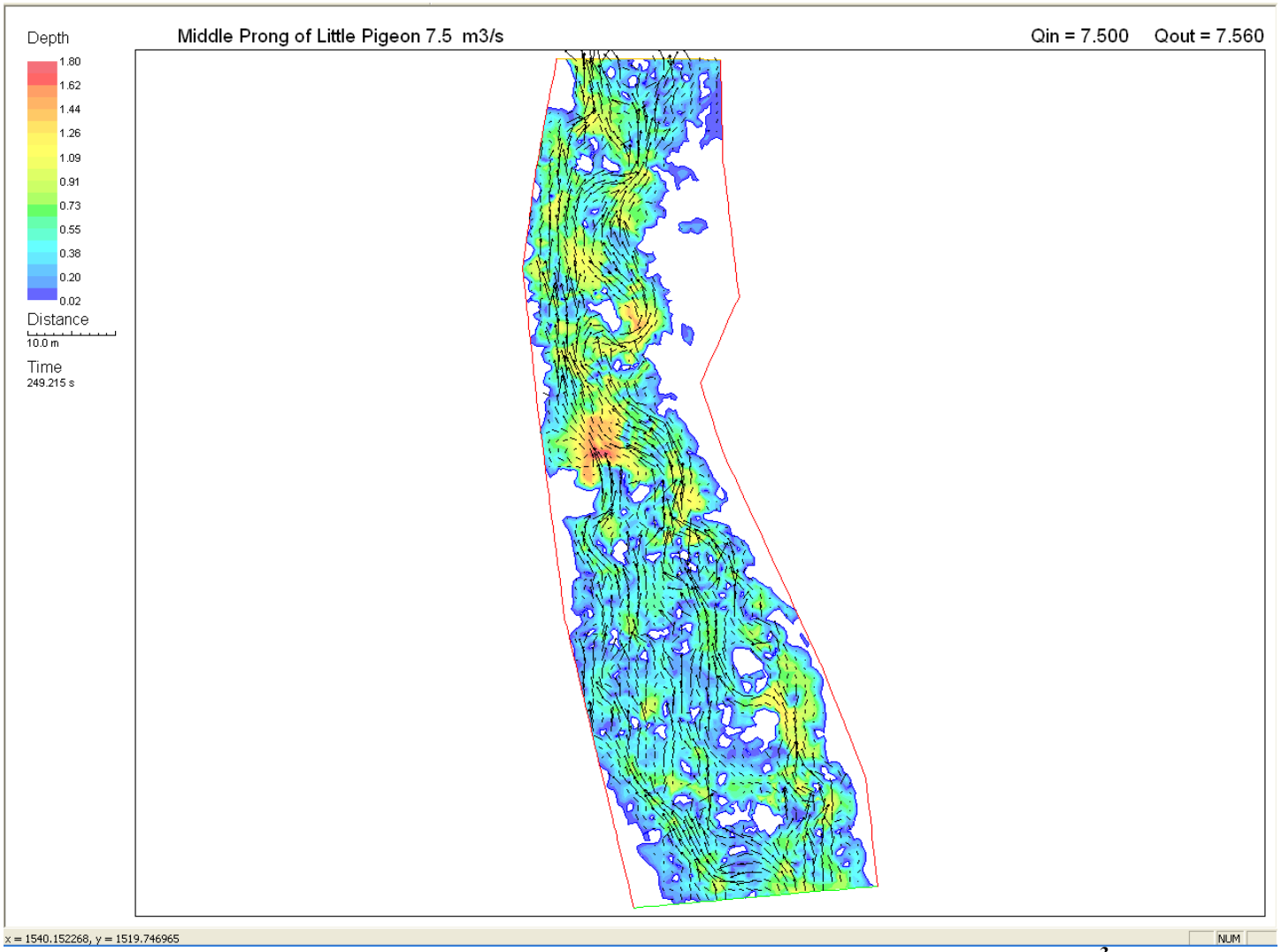

Figure 6. River2D results for depth at Middle Prong site for discharge of 7.5 m^3/s

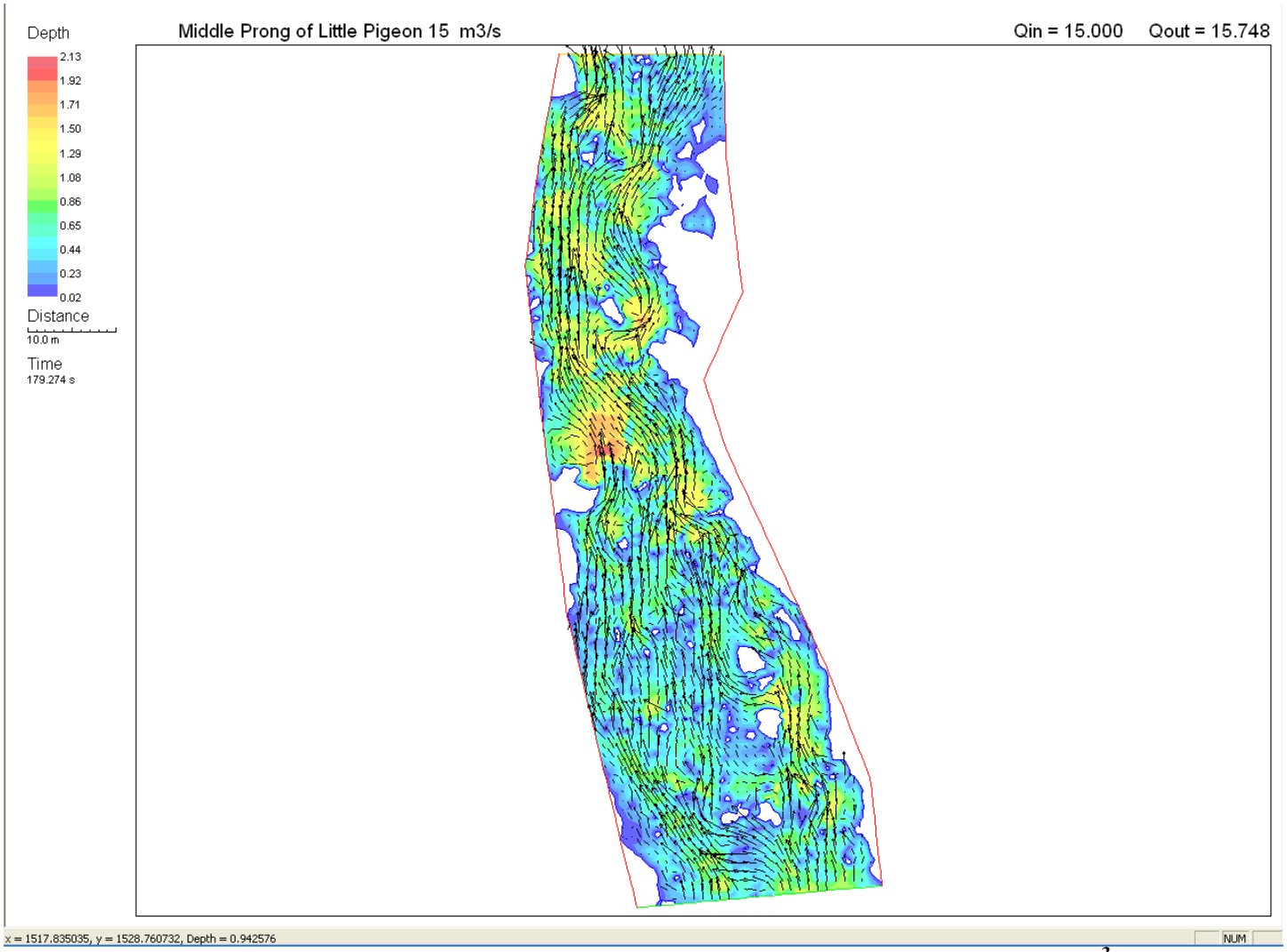

Figure 7. River2D results for depth at Middle Prong site for discharge of 15 m^3/s

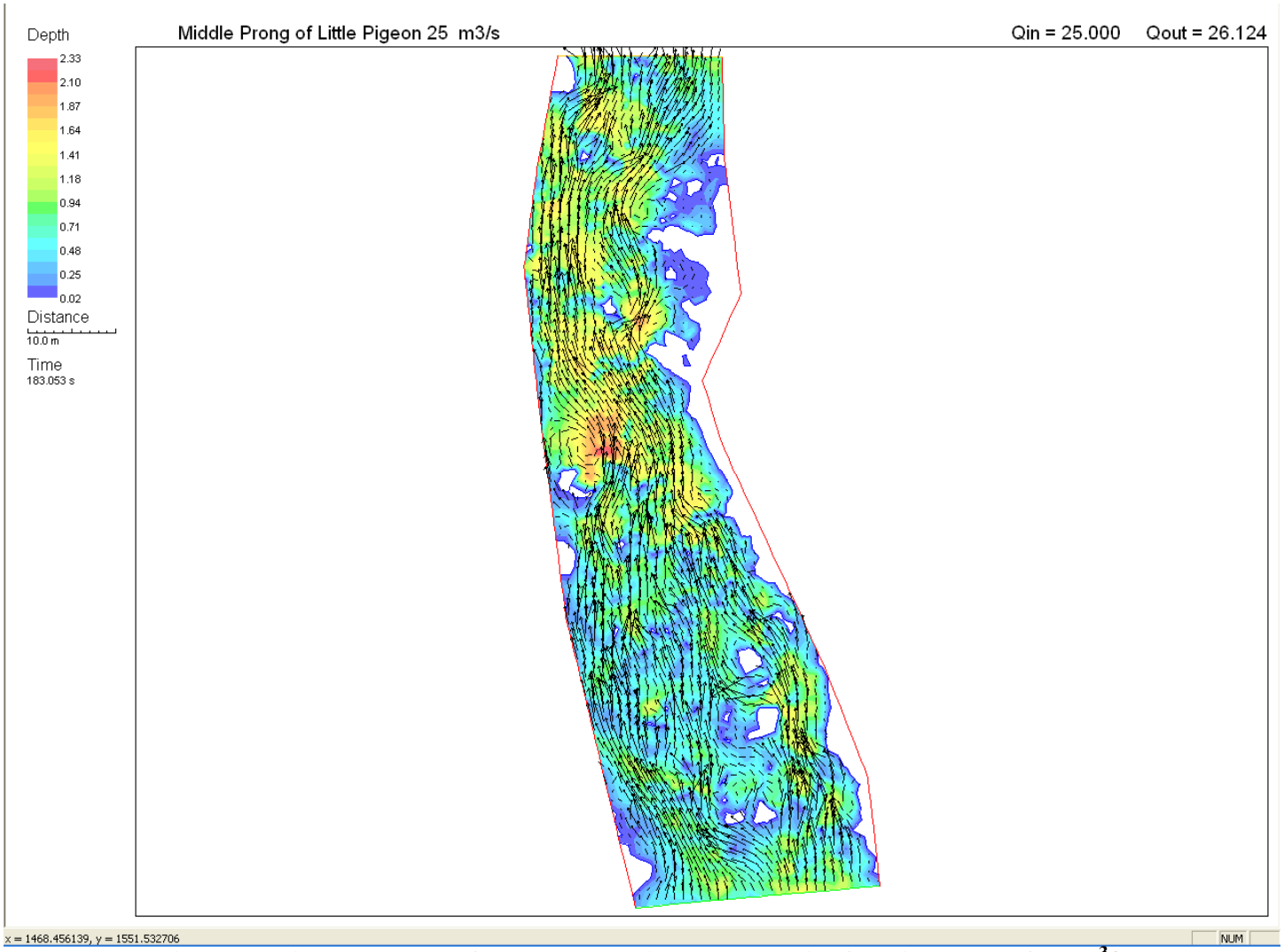

Figure 8. River2D results for depth at Middle Prong site for discharge of 25 m^3/s

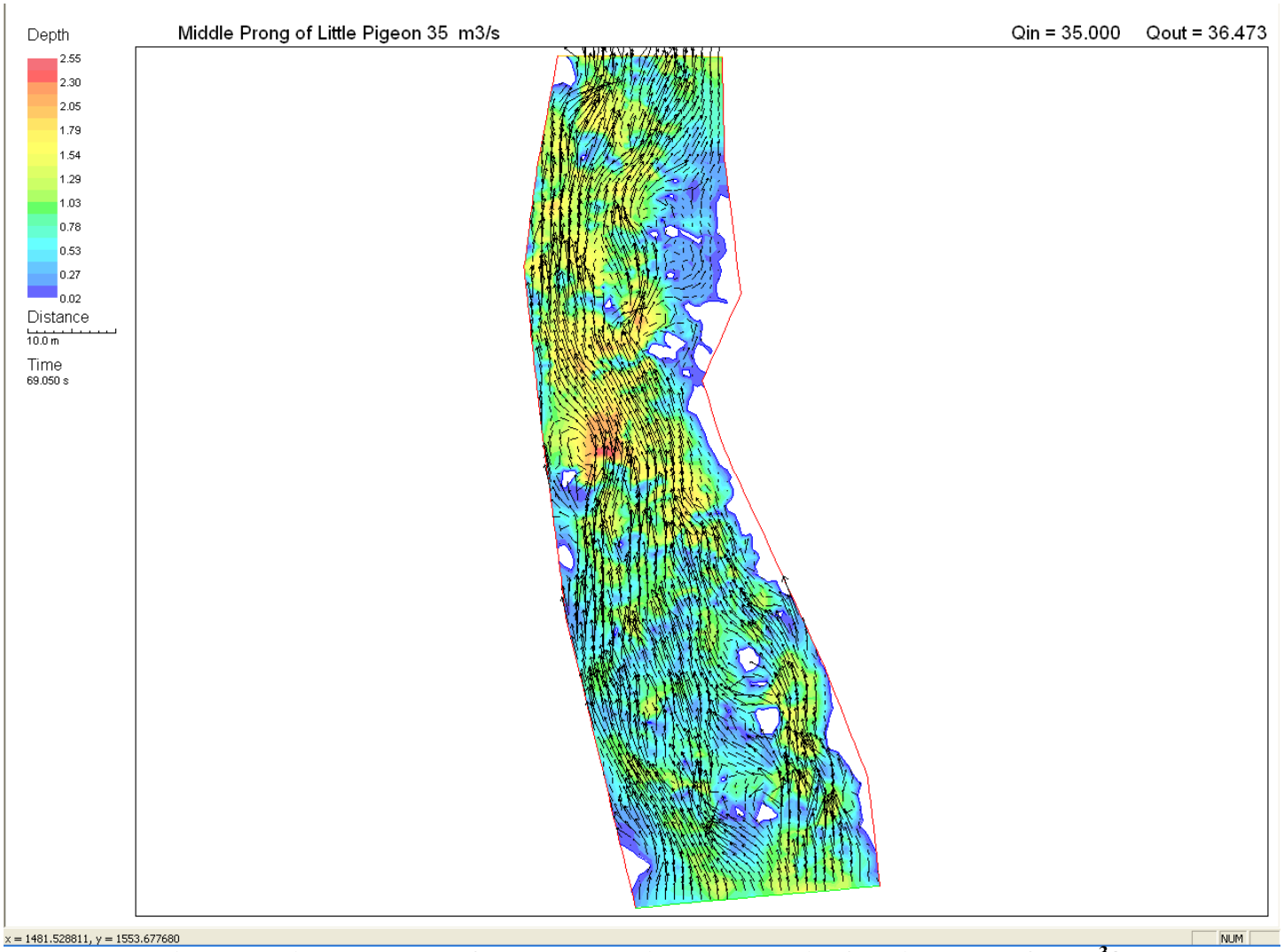

Figure 9. River2D results for depth at Middle Prong site for discharge of 35 m^3/s

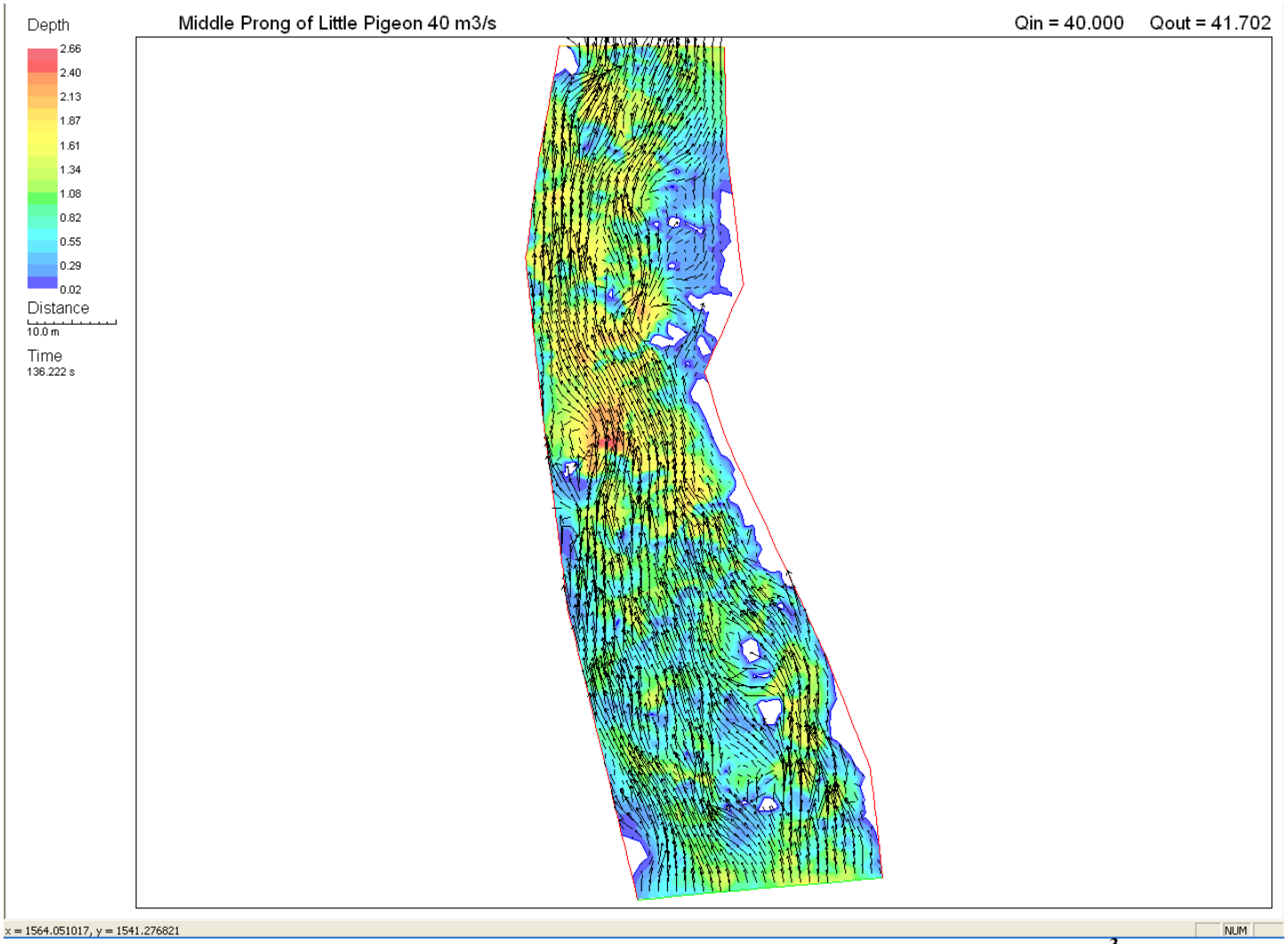

Figure 10. River2D results for depth at Middle Prong site for discharge of 40 m^3/s

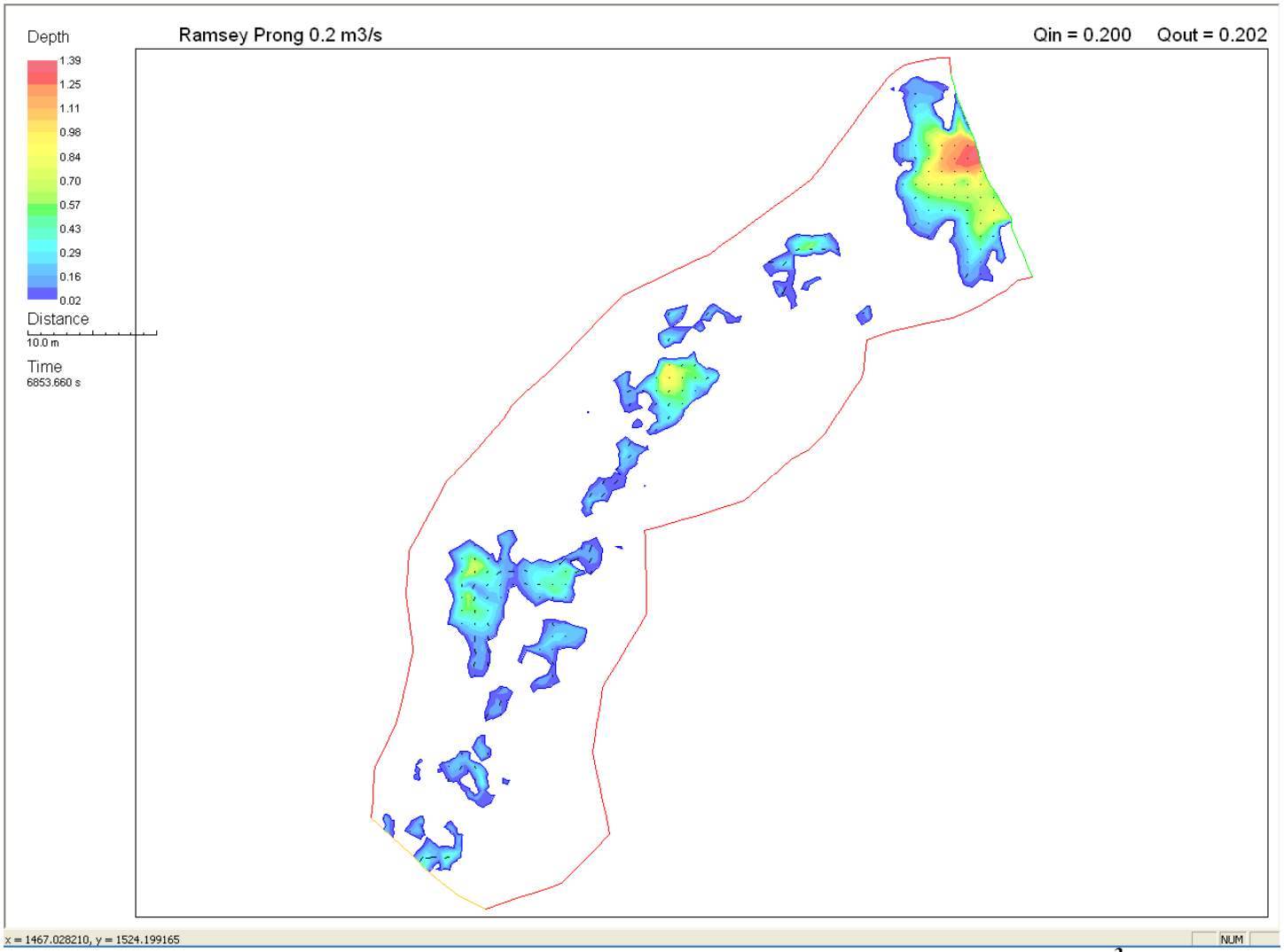

Figure 11. River2D results for depth at Ramsey Prong site for discharge of 0.2 m^3/s

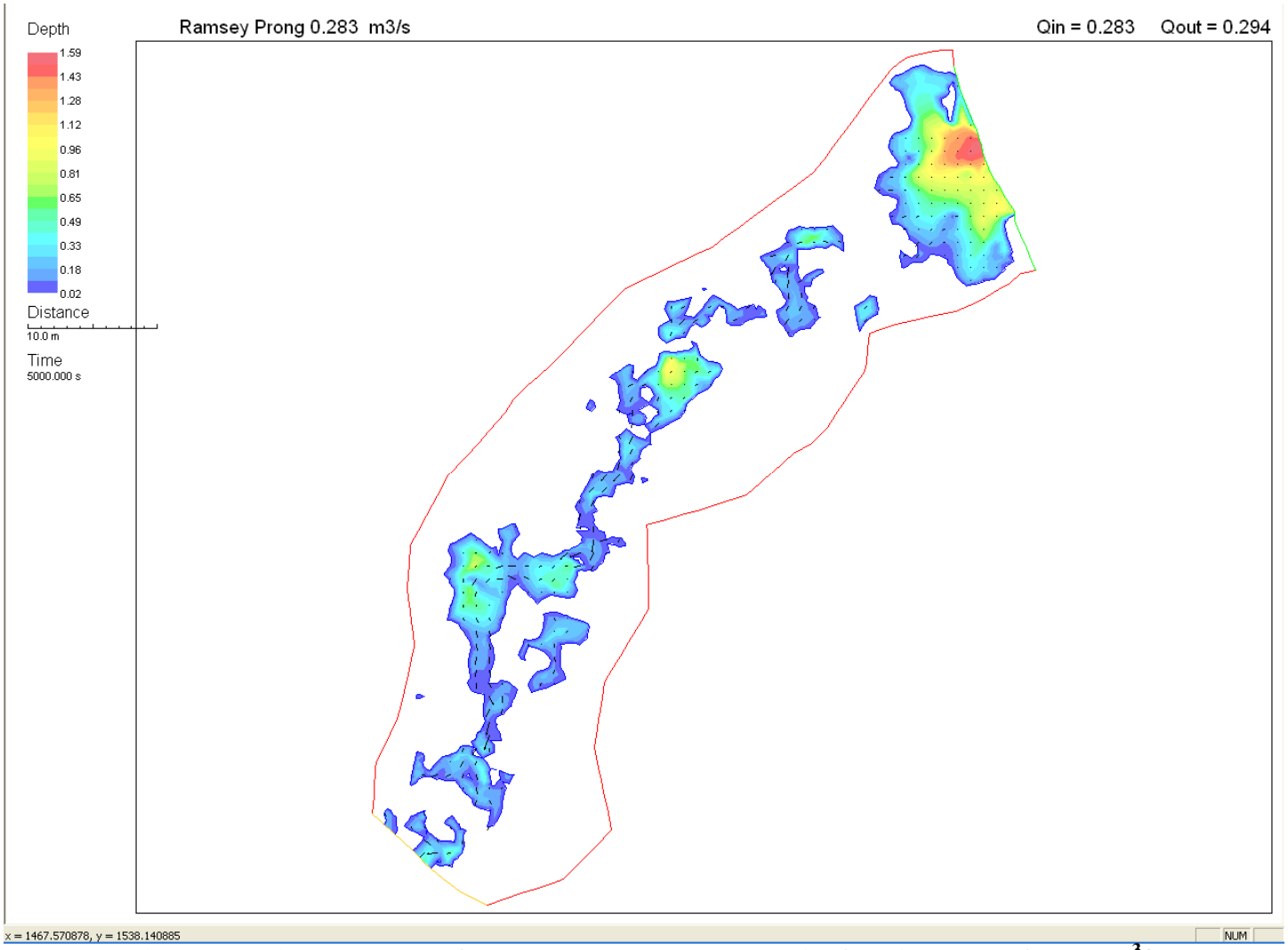

Figure 12. River2D results for depth at Ramsey Prong site for discharge of 0.283 m^3/s

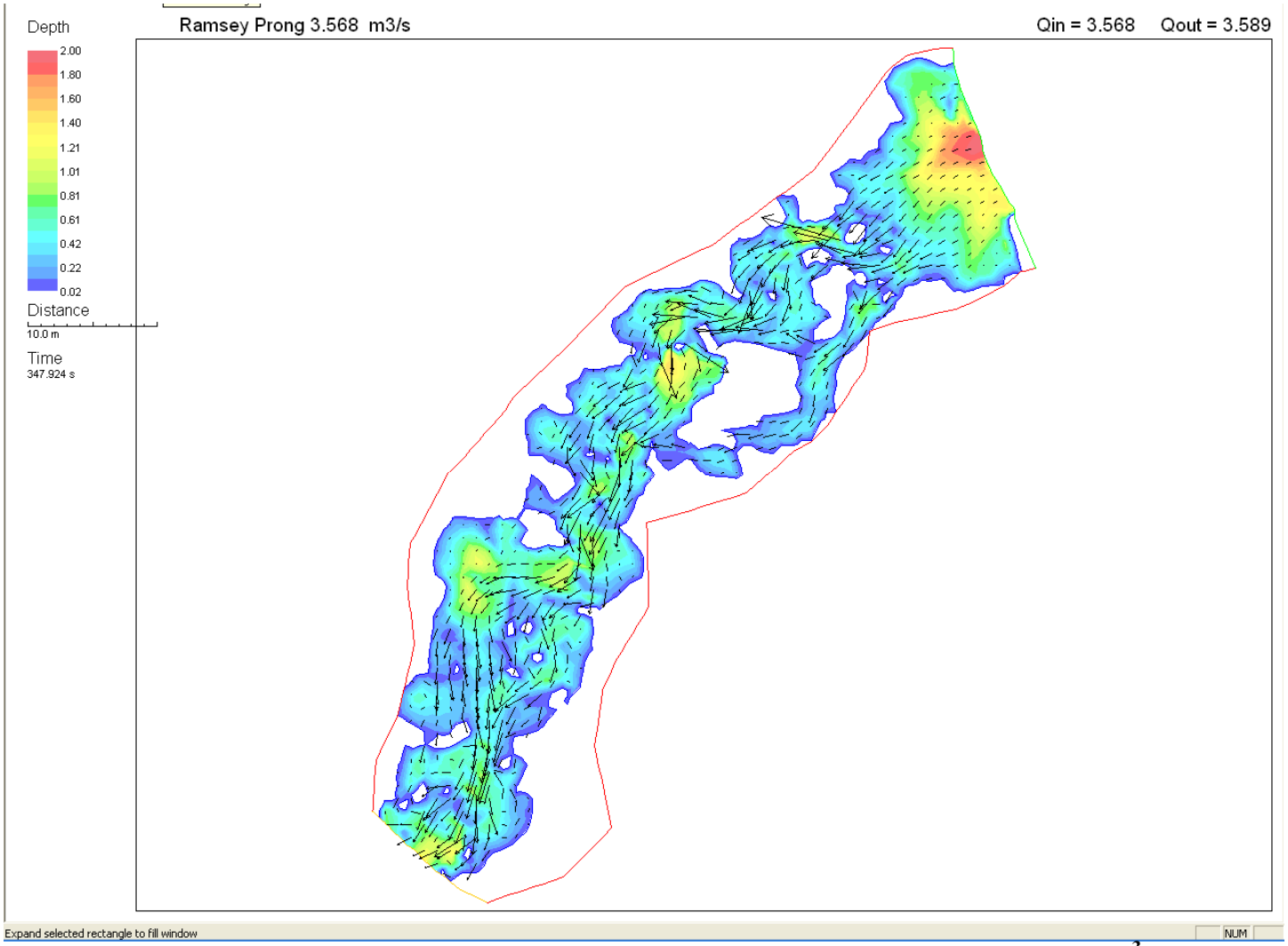

Figure 13. River2D results for depth at Ramsey Prong site for discharge of 3.568 m^3/s

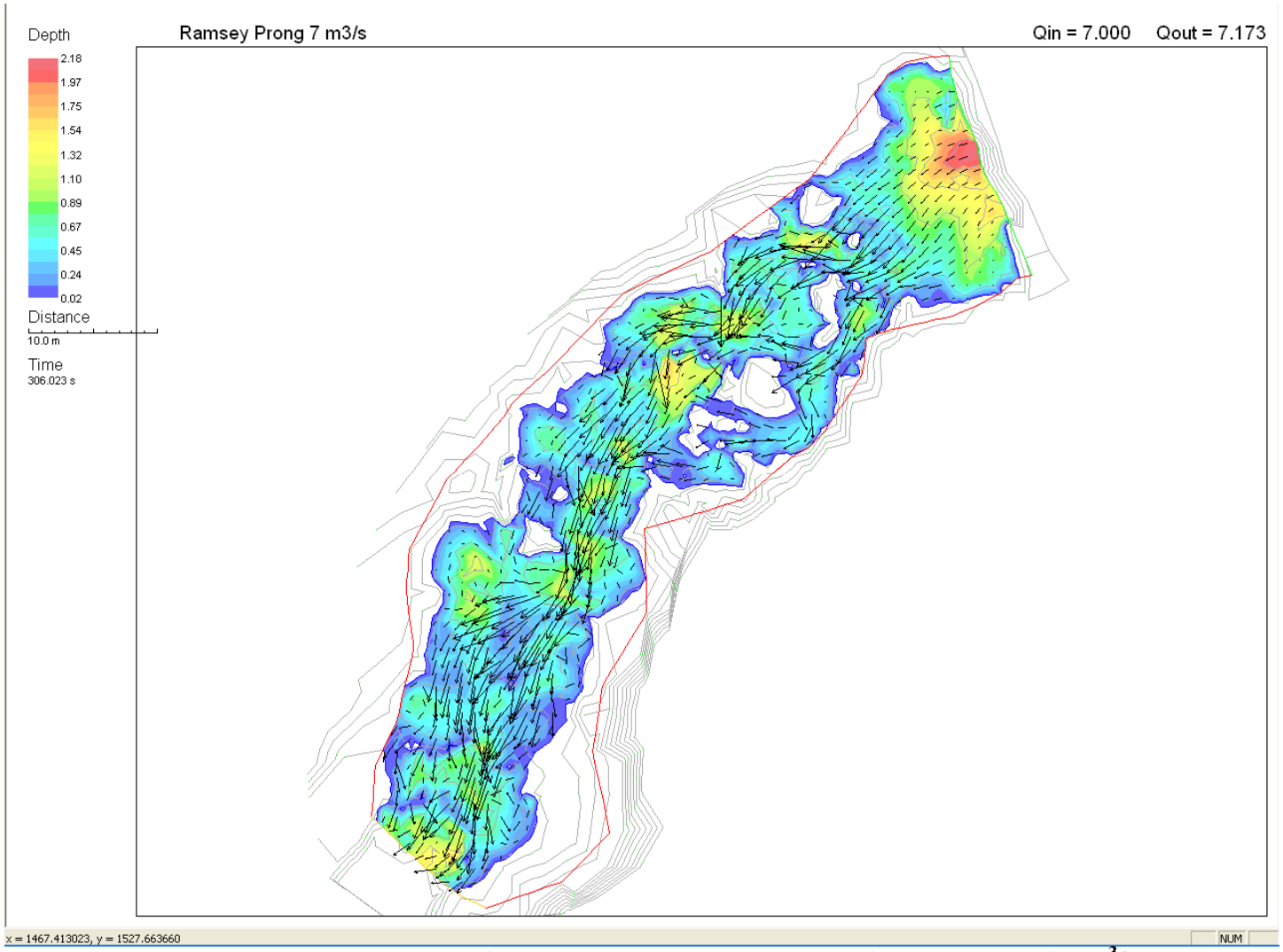

Figure 14. River2D results for depth at Ramsey Prong site for discharge of 7 m^3/s

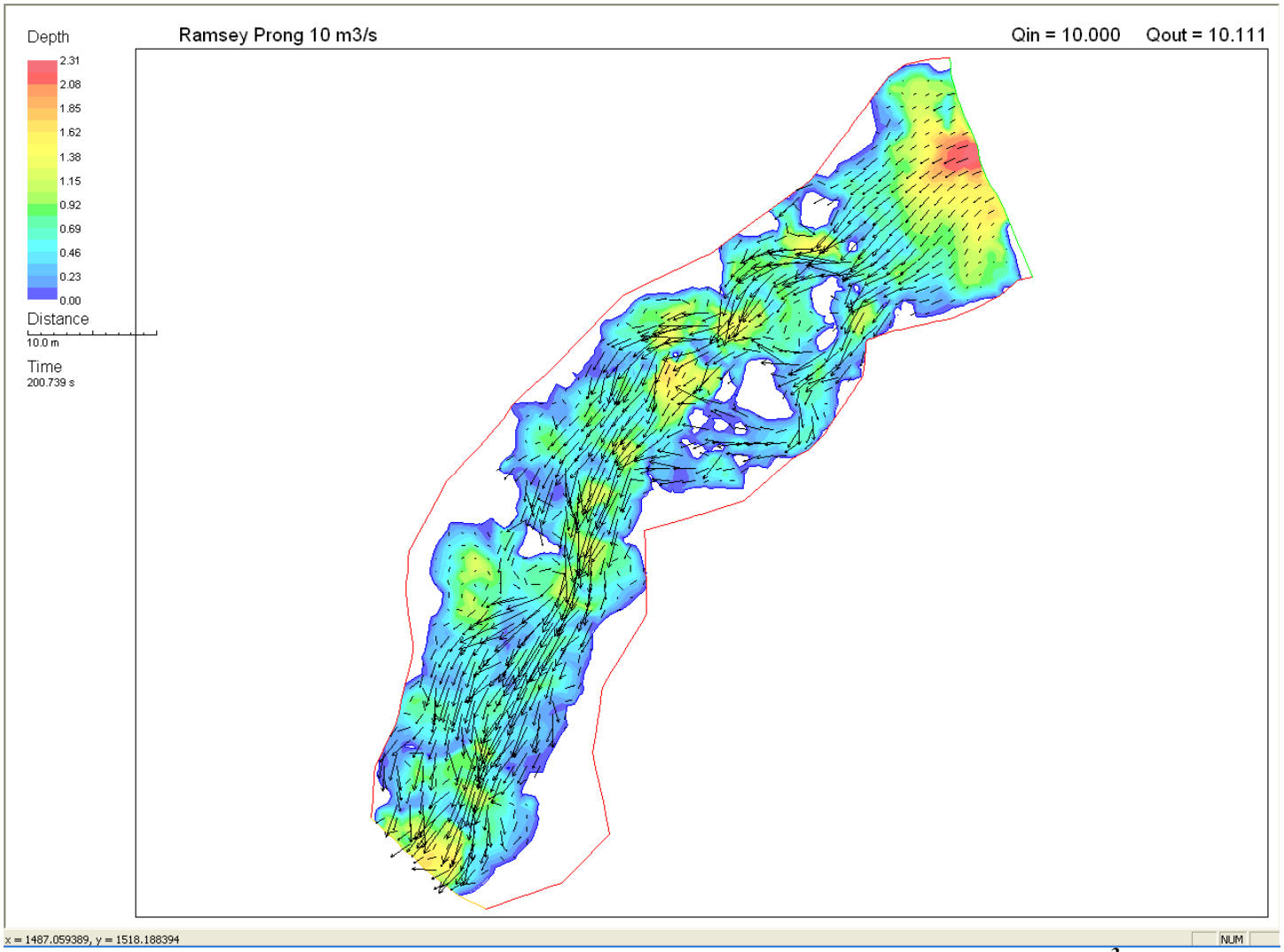

Figure 15. River2D results for depth at Ramsey Prong site for discharge of 10 m^3/s

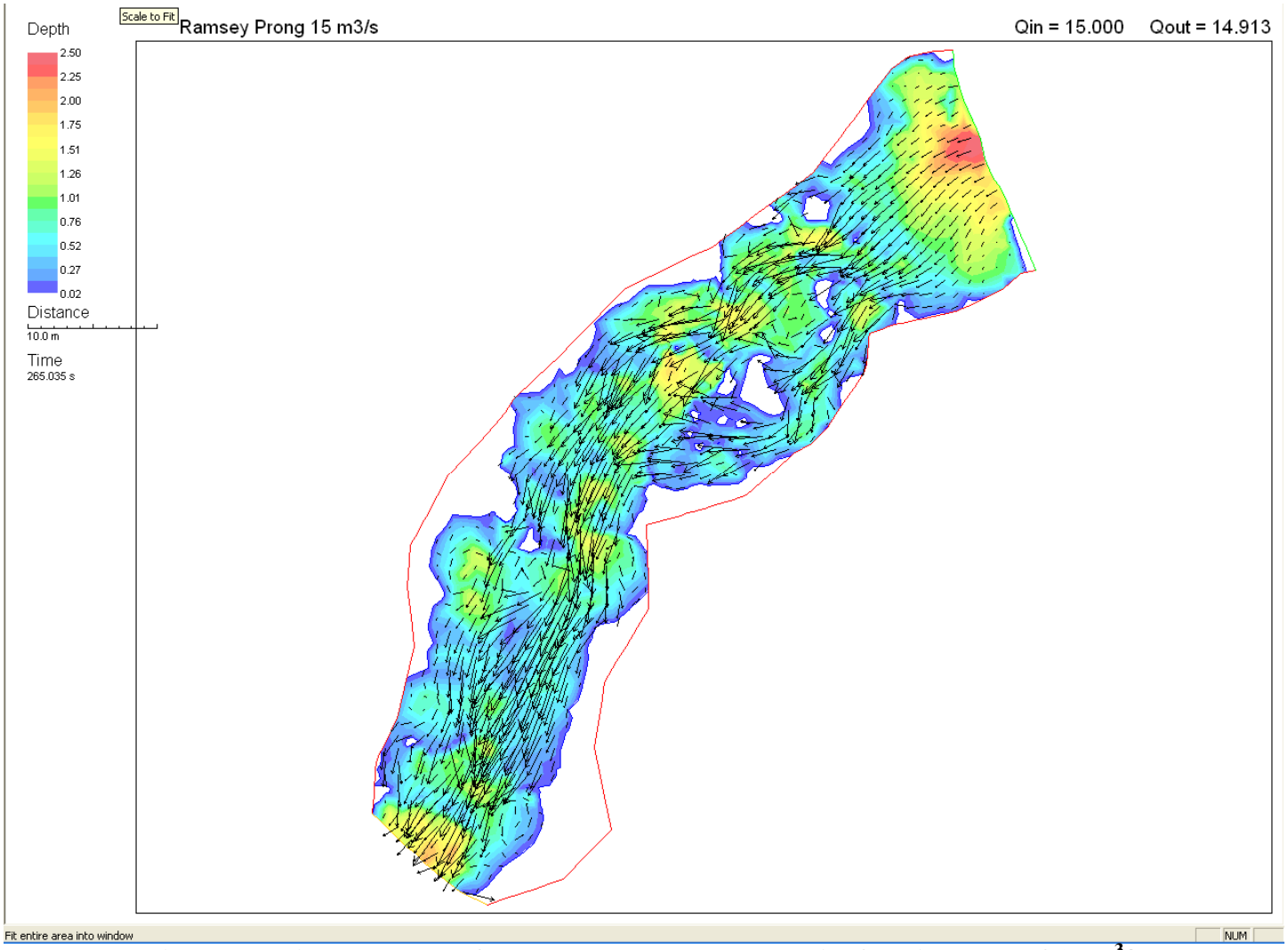

Figure 16. River2D results for depth at Ramsey Prong site for discharge of 15 m^3/s

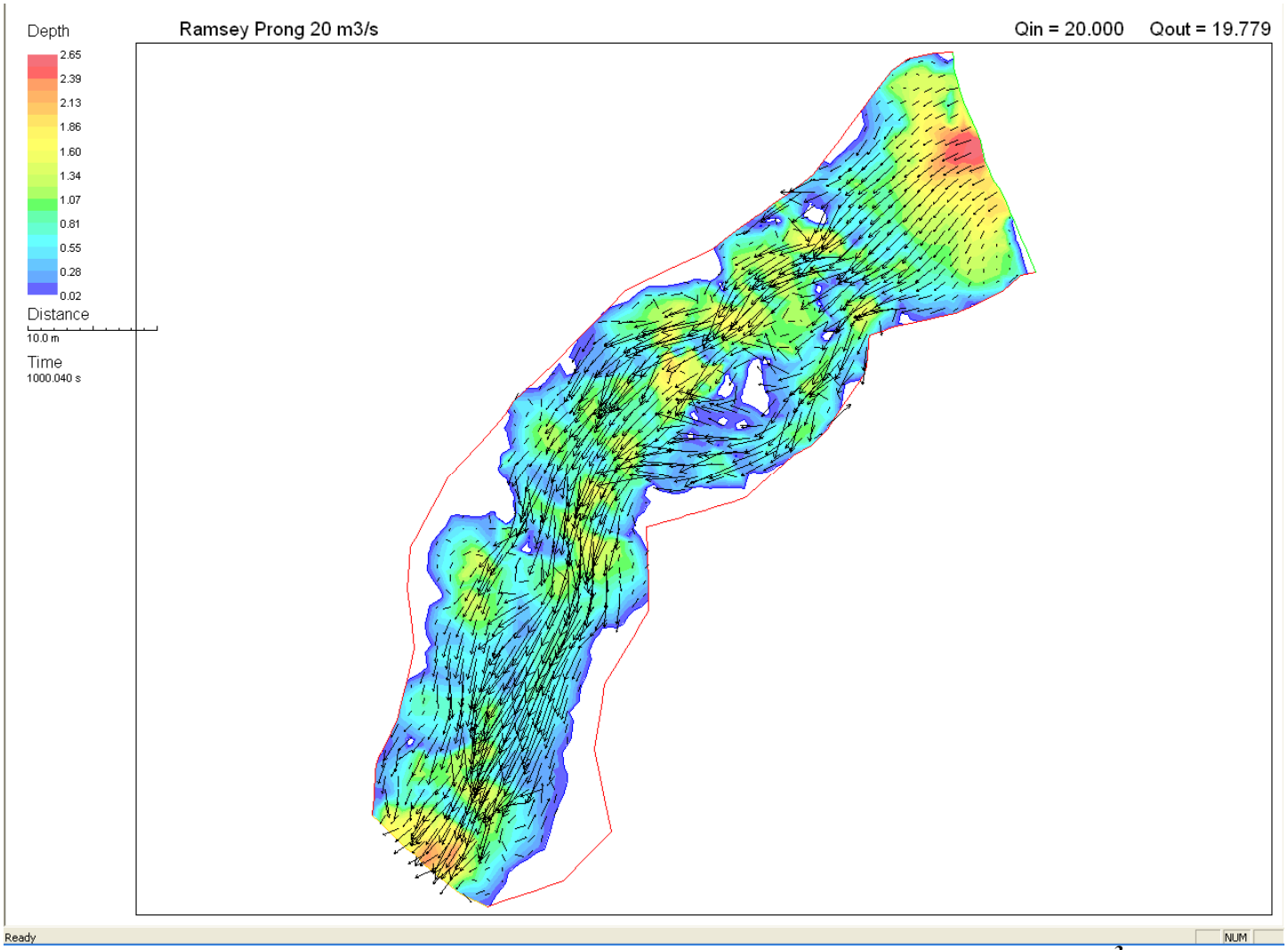

Figure 17. River2D results for depth at Ramsey Prong site for discharge of 20 m^3/s

Appendix C: Stage-Discharge Relationships

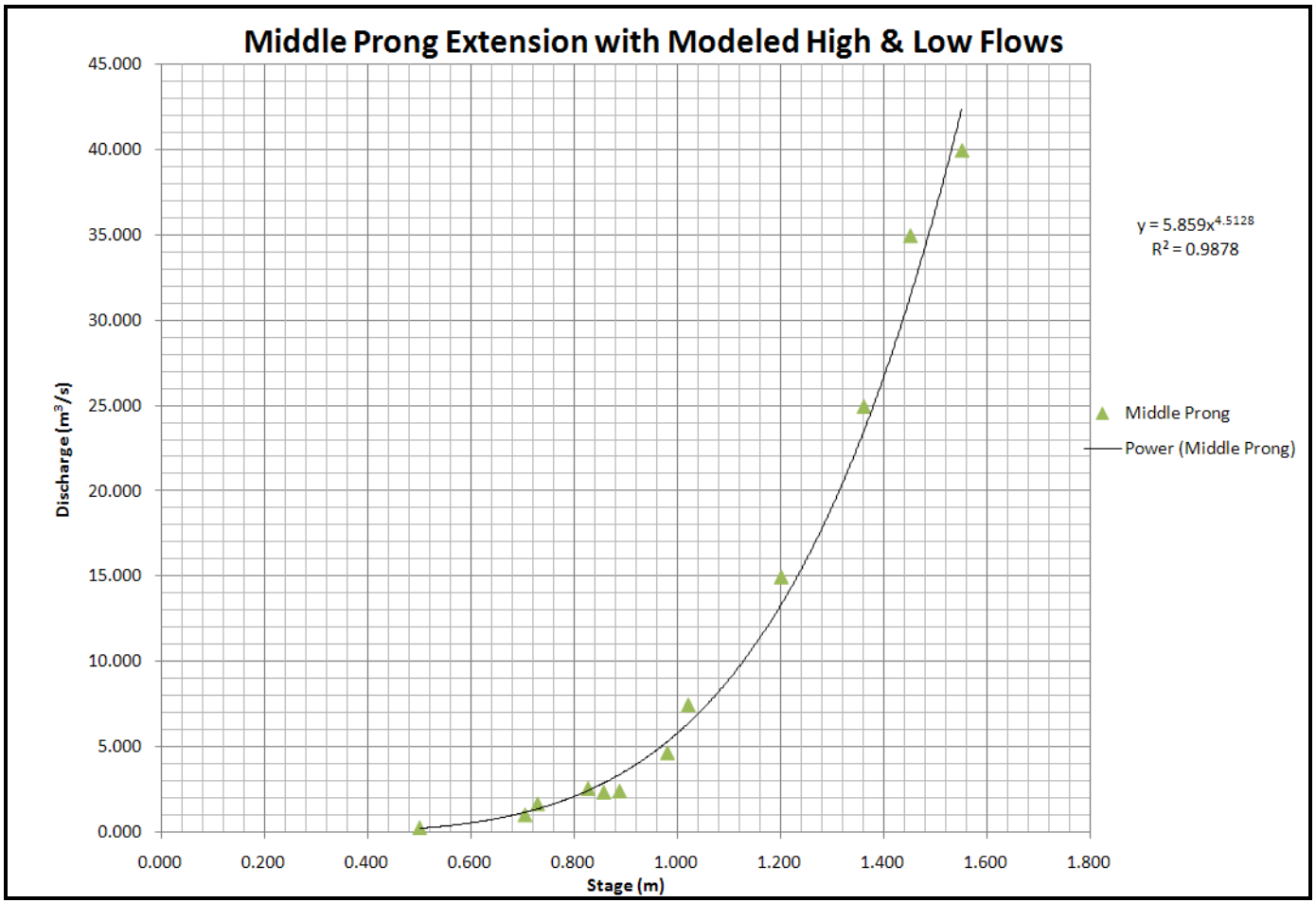

Figure 18. Middle Prong site stage-discharge relationship

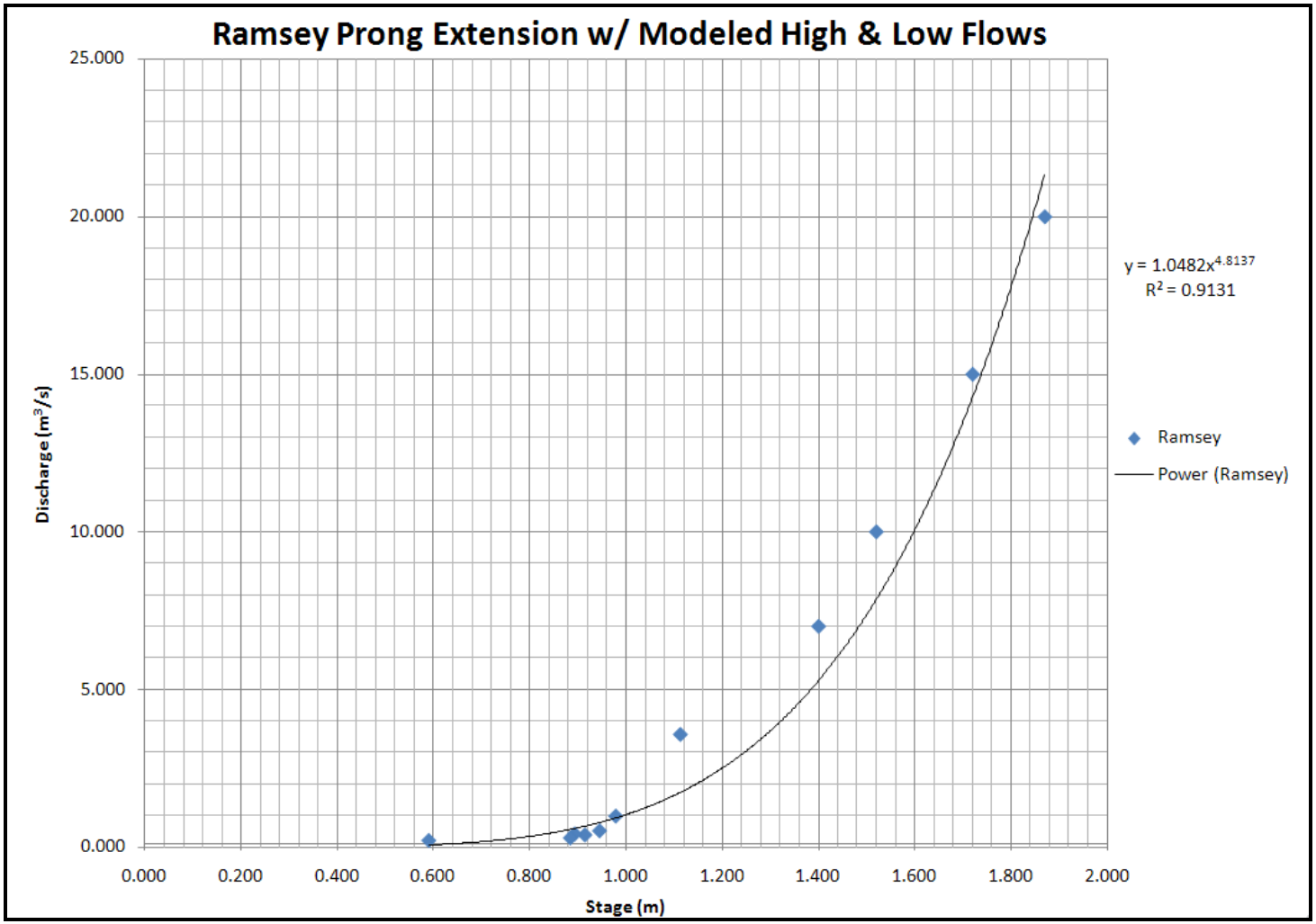

Figure 19. Ramsey Prong site stage-discharge relationship

Appendix D: Regression Equations

Ion	M1			M2		
	Regression Equation	r^2	p	Regression Equation	r^2	p
Cl eq	y= 0.0111x + 0.8799	0.9235	< 0.01	y = .008x + 1.9187	0.6458	< 0.01
Dormant NO3-N eq	y = 0.062x – 44.4	0.9230	< 0.01	y=0.0695x-8.2698	0.8080	< 0.01
Transpiration NO3-N eq	y = 0.0343x + 7.119	0.9379	< 0.01	y=0.0262x + 2.2506	0.7910	< 0.01
SO4 eq	y = 0.052x + 2.1799	0.9645	< 0.01	y = 0.0432x + 0.7824	0.8982	< 0.01
NH4-N eq	y = 0.0018x – 1.0112	0.6219	< 0.01	y = -0.0006x + 1.0555	0.0301	0.17
Na eq	y = 0.0229x + 1.4419	0.9468	< 0.01	y = 0.0225x + 1.9591	0.9100	< 0.01
K eq	y = 0.0112x + 2.4025	0.7434	< 0.01	y = 0.013x – 0.1137	0.7332	< 0.01
Mg eq	y= 0.0297x – 4.7363	0.9549	< 0.01	y = 0.0226x -0.6544	0.8967	< 0.01
Ca, eq	y = 0.0621x – 11.633	0.9646	< 0.01	y = 0.0568x – 3.1155	0.8794	< 0.01

Table 10. Mass regression equations for M1 and M2

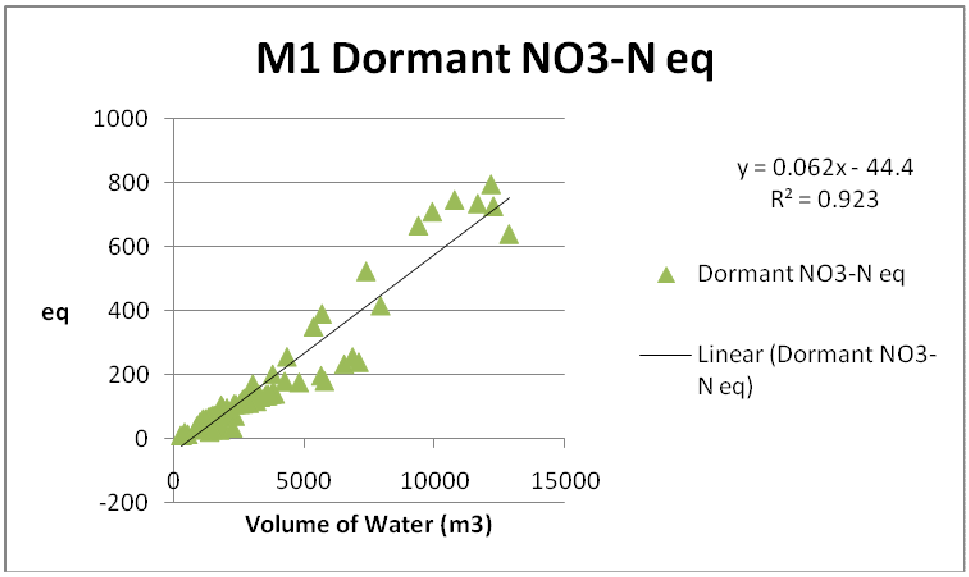

Figure 20. Middle Prong site dormant NO_3^- regression

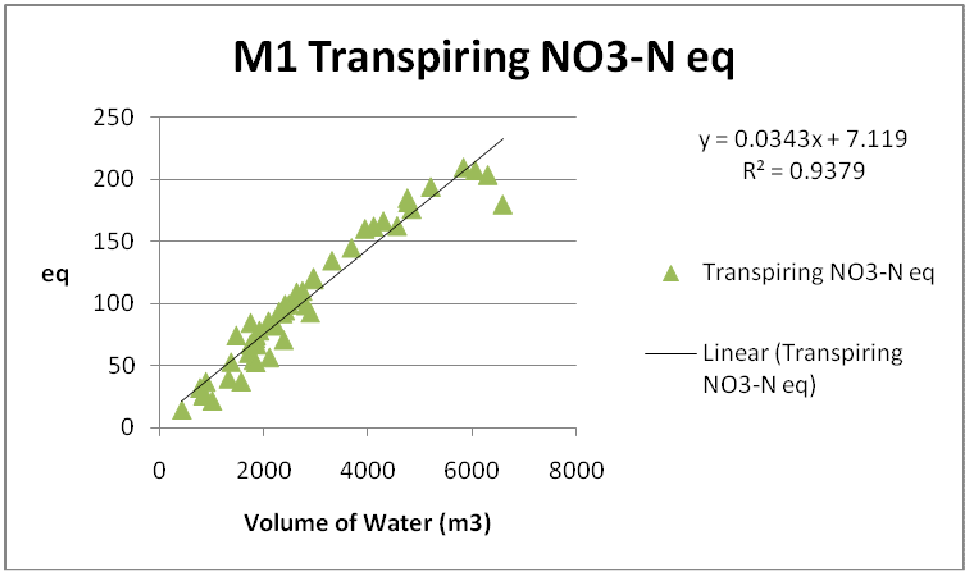

Figure 21. Middle Prong site transpiring NO_3^- regression

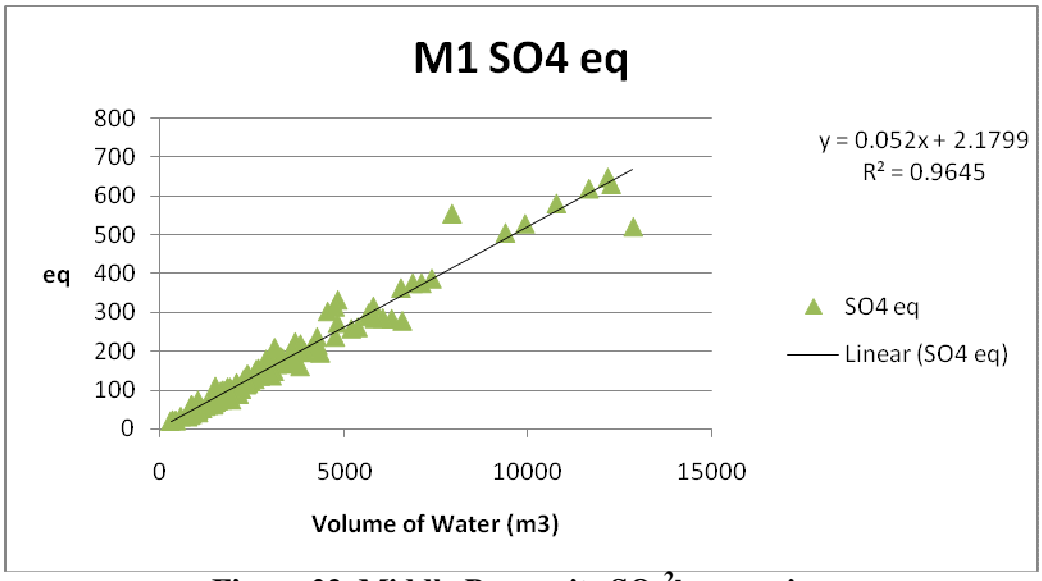

Figure 22. Middle Prong site SO_4^{2-} regression

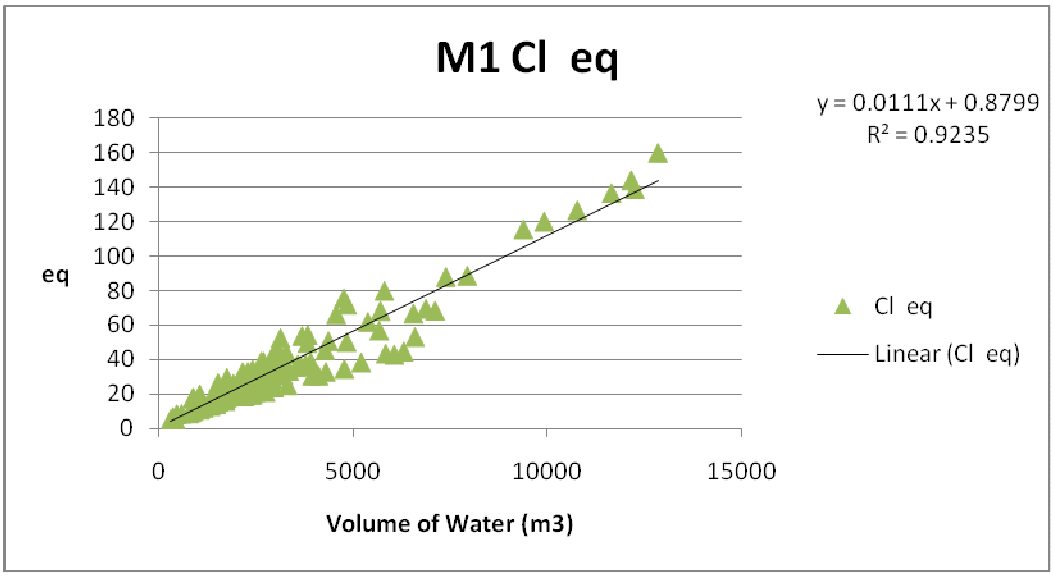

Figure 23. Middle Prong site Cl^- regression

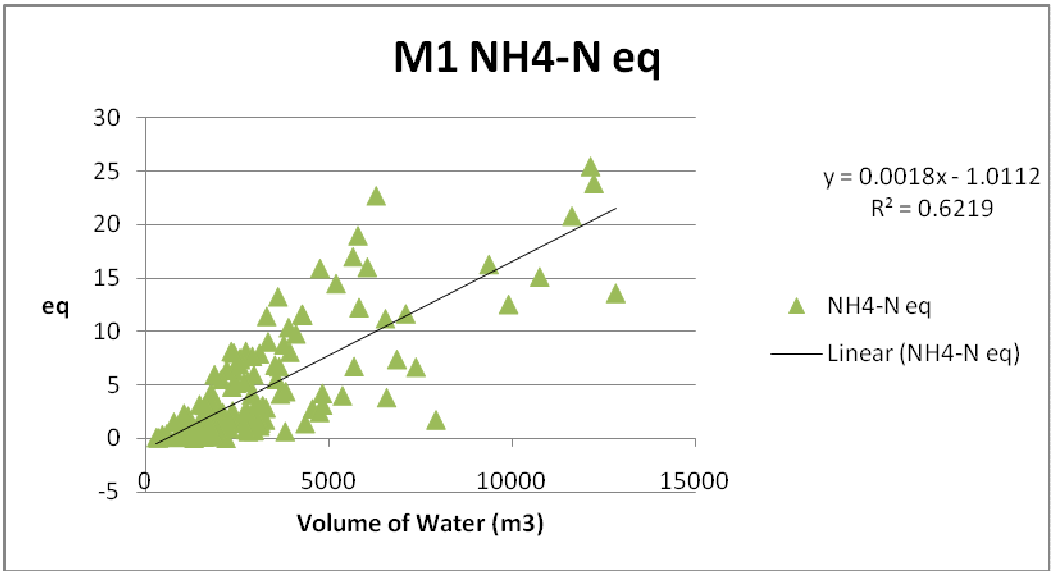

Figure 24. Middle Prong site NH_4^+ regression

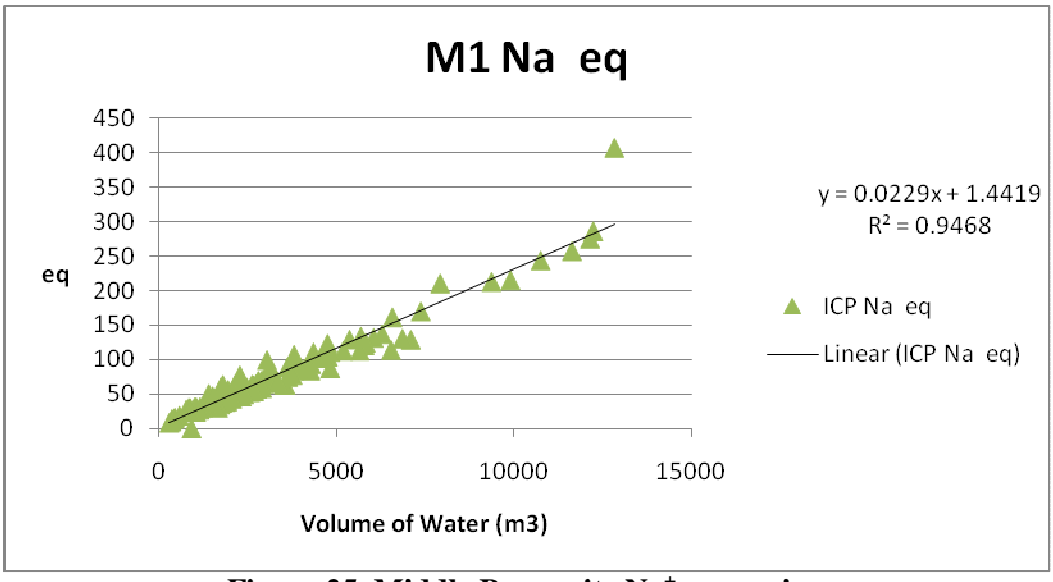

Figure 25. Middle Prong site Na^+ regression

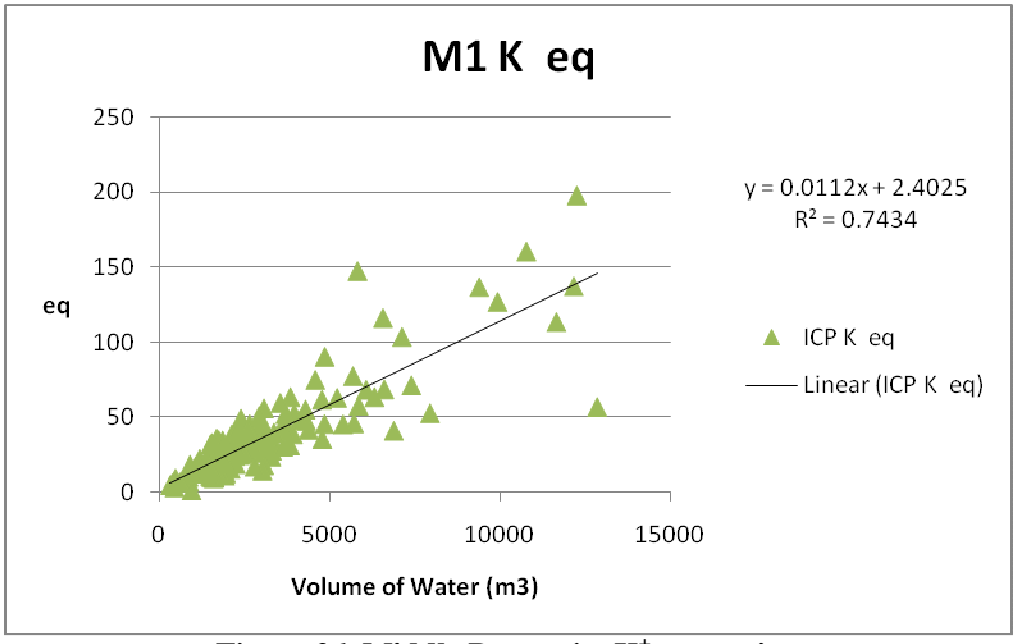

Figure 26. Middle Prong site K^+ regression

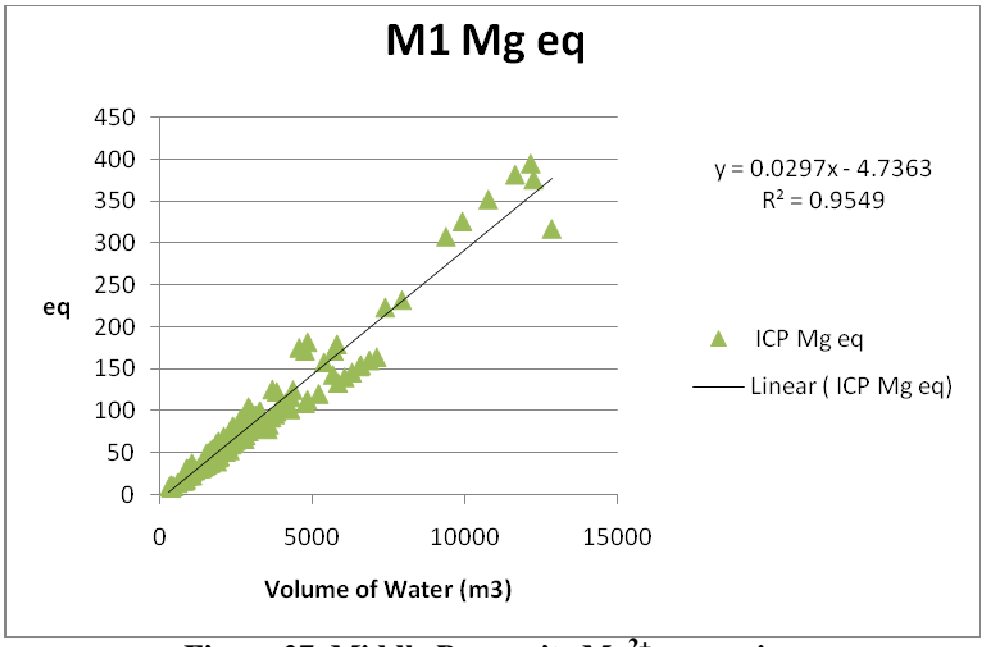

Figure 27. Middle Prong site Mg^{2+} regression

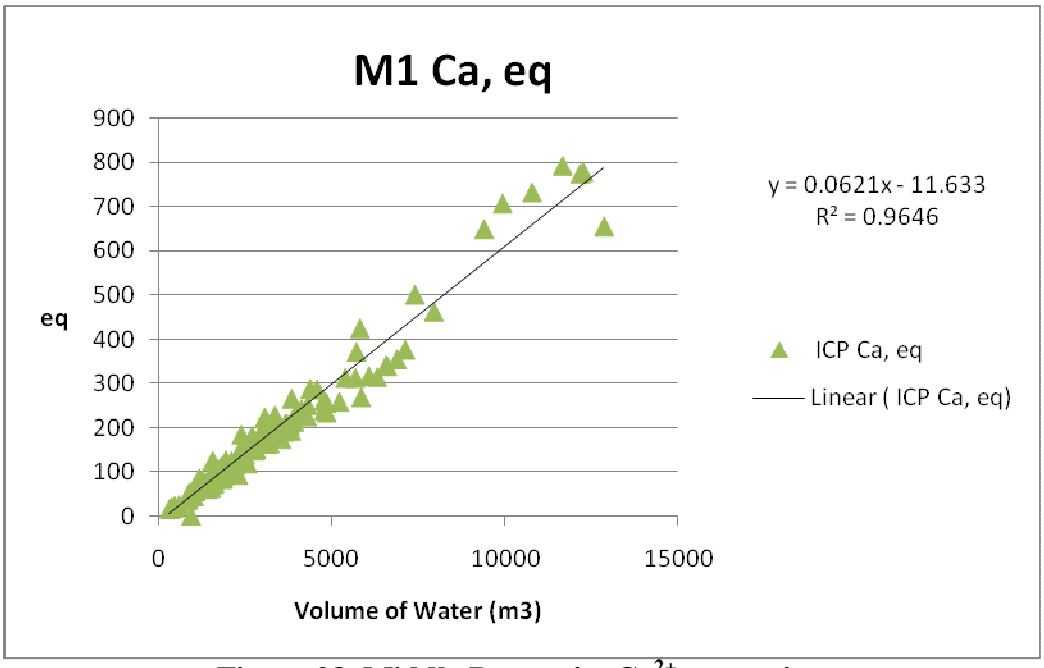

Figure 28. Middle Prong site Ca^{2+} regression

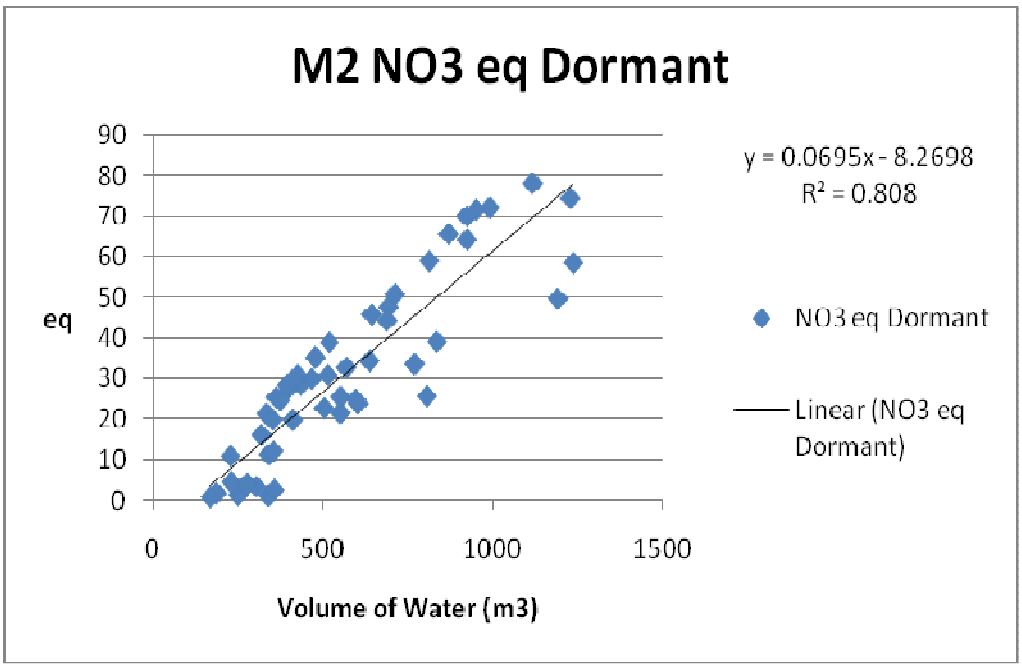

Figure 29. Ramsey Prong site dormant NO_3^- regression

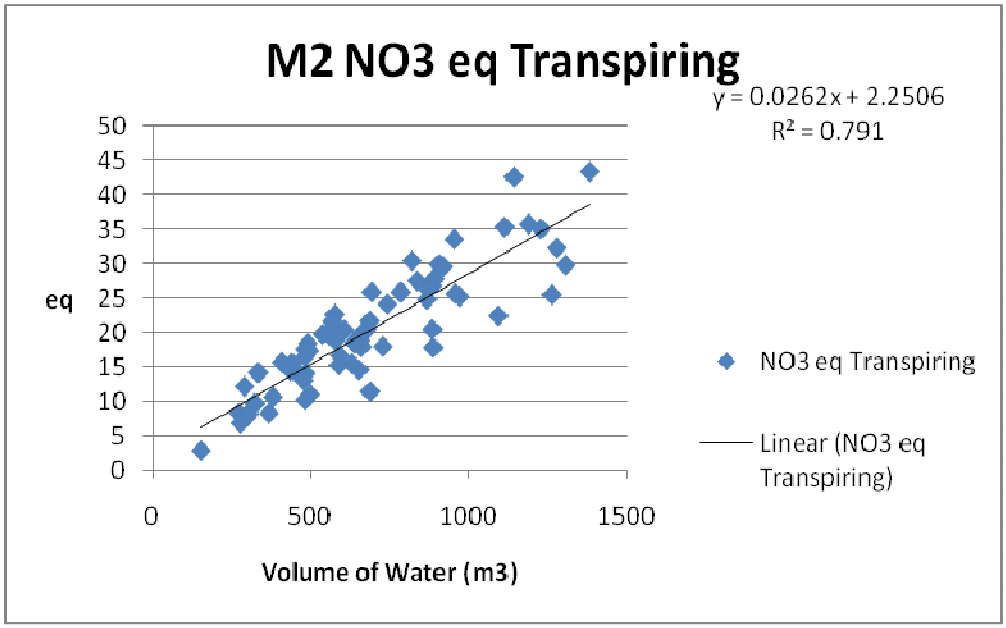

Figure 30. Ramsey Prong site transpiring NO_3^- regression

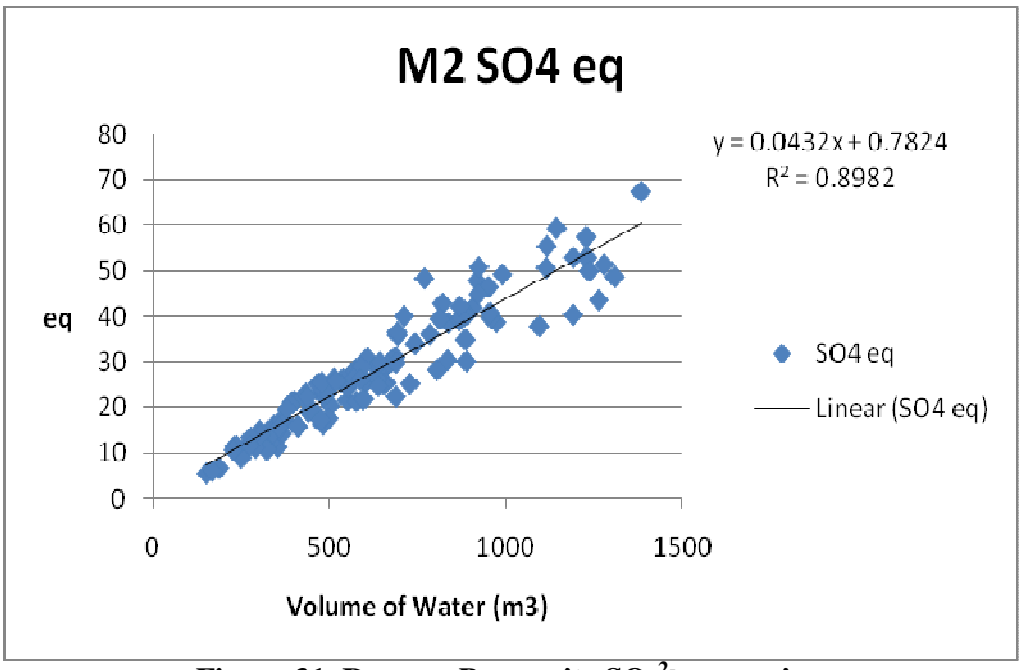

Figure 31. Ramsey Prong site SO_4^{2-} regression

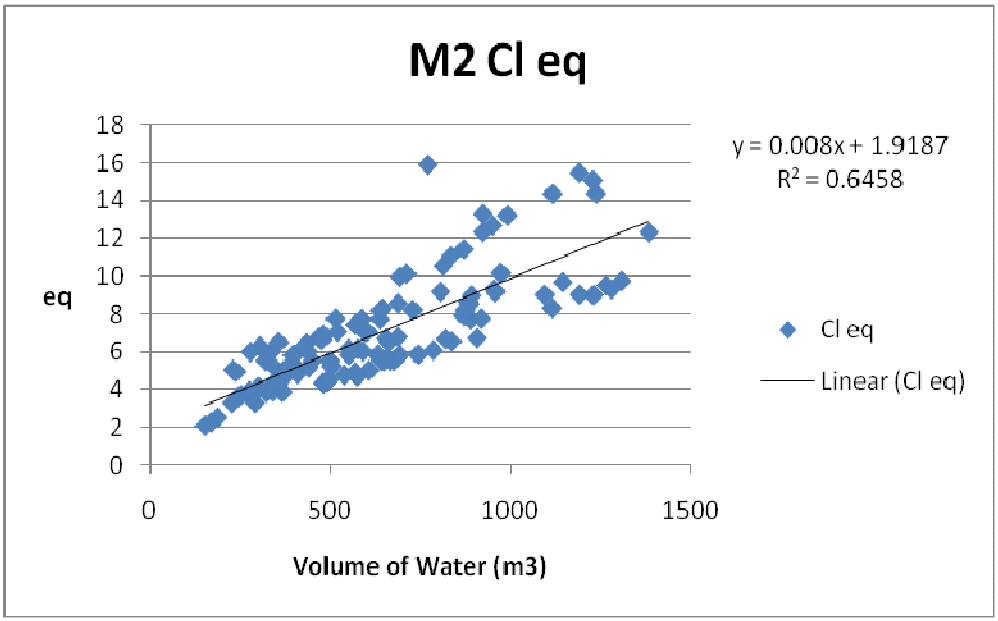

Figure 32. Ramsey Prong site Cl^- regression

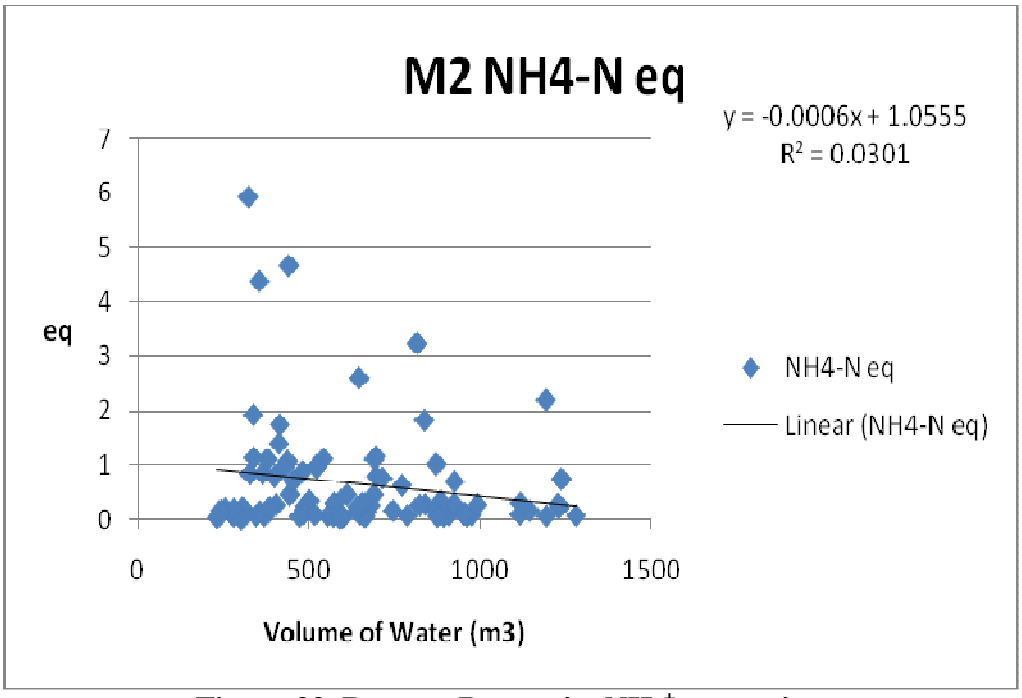

Figure 33. Ramsey Prong site NH_4^+ regression

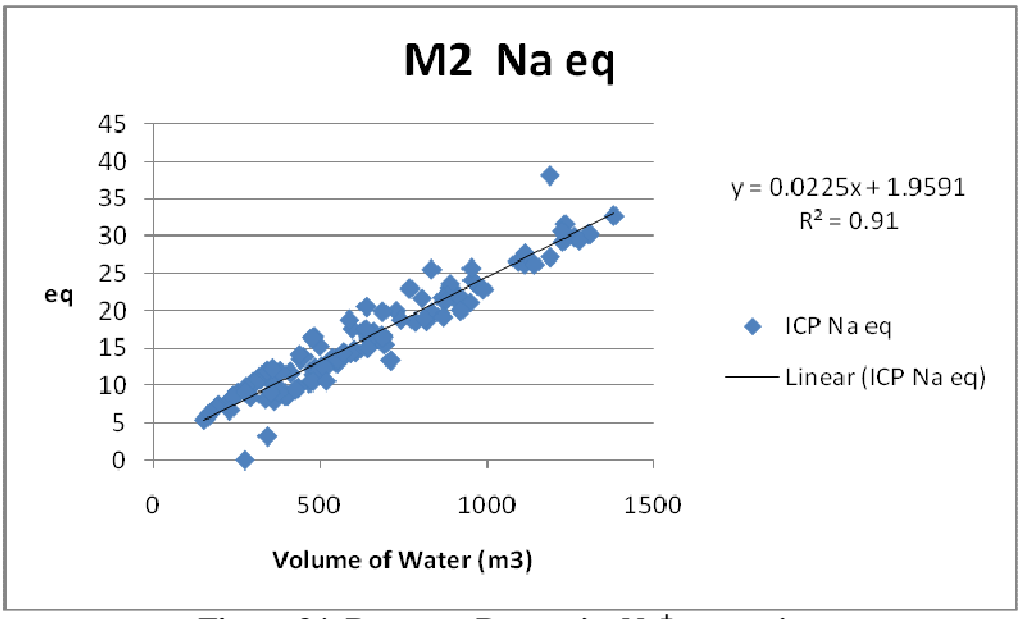

Figure 34. Ramesey Prong site Na^+ regression

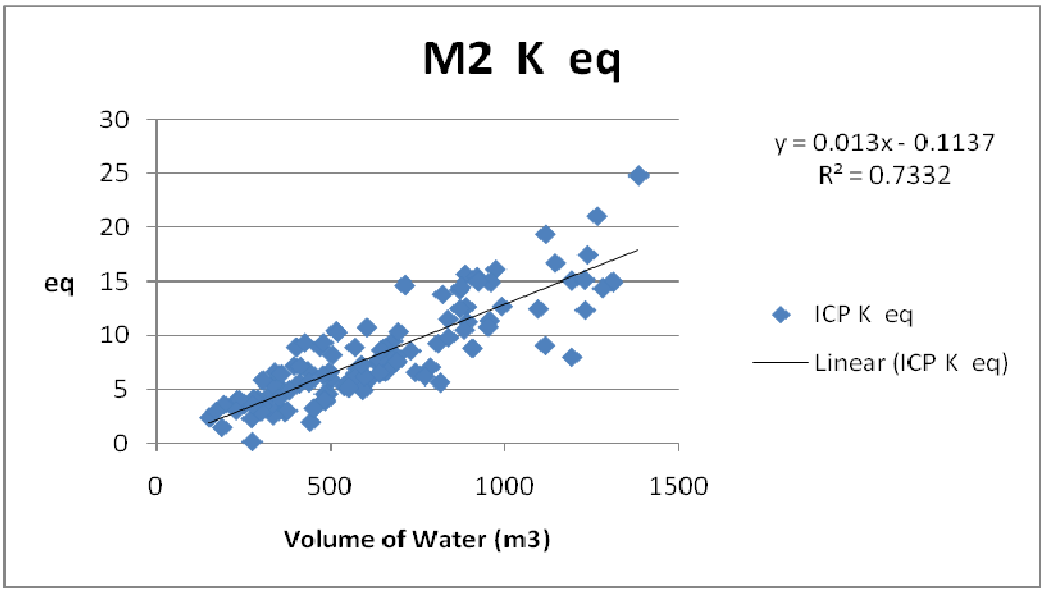

Figure 35. Ramsey Prong site K^+ regression

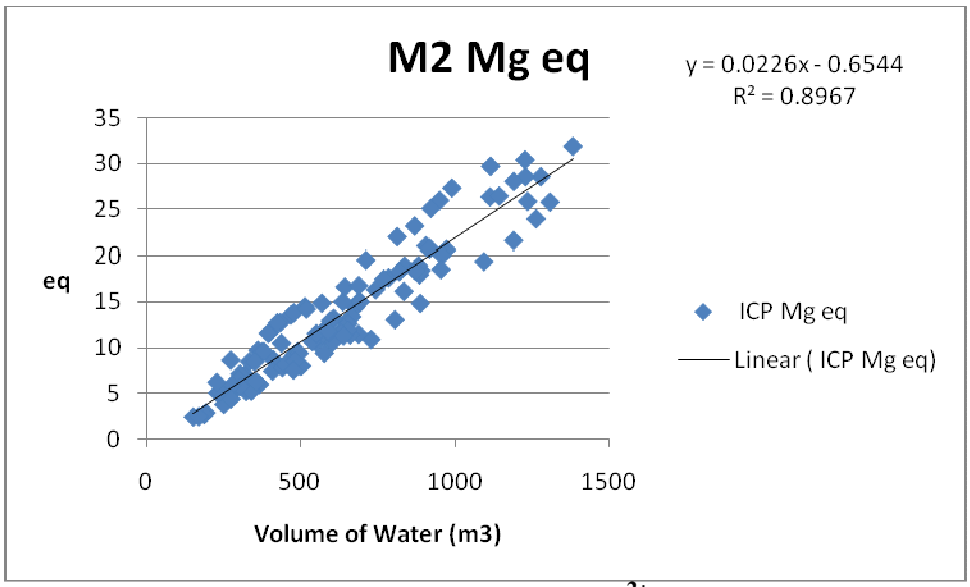

Figure 36. Ramsey Prong site Mg^{2+} regression

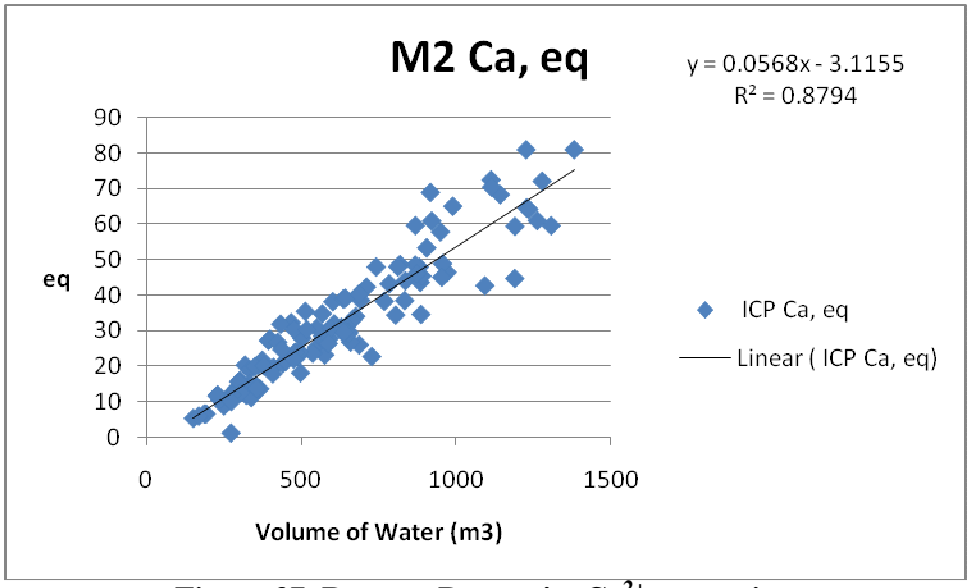

Figure 37. Ramsey Prong site Ca^{2+} regression

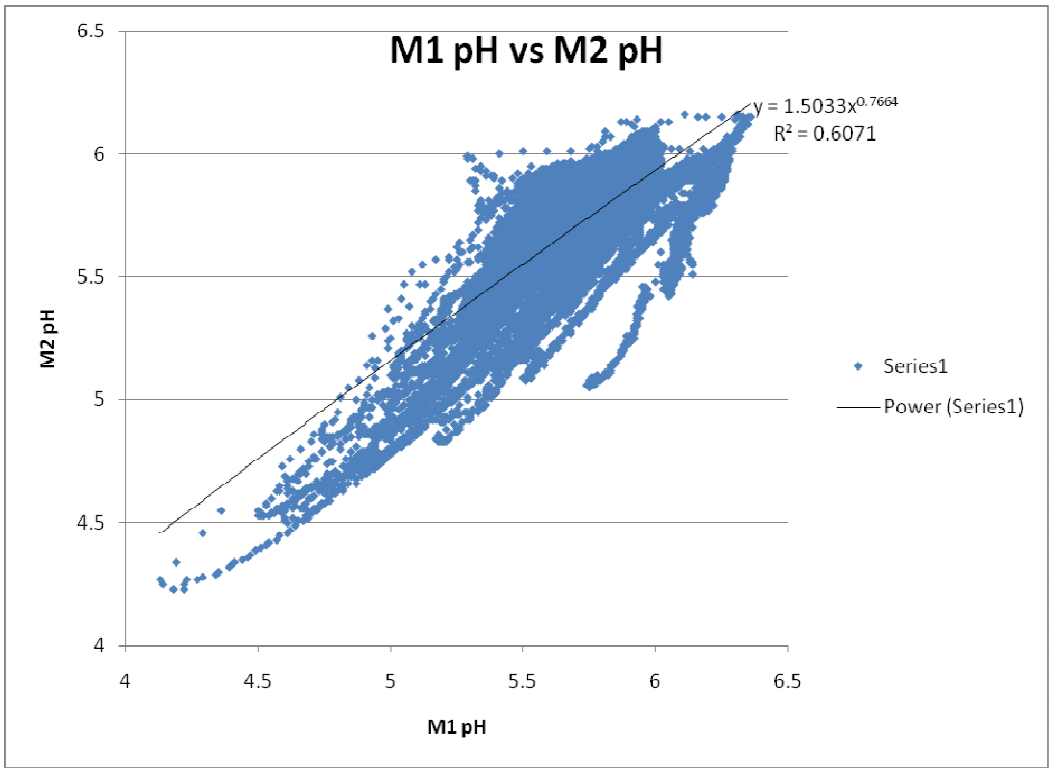

Figure 38. Middle Prong pH vs. Ramsey Prong pH regression

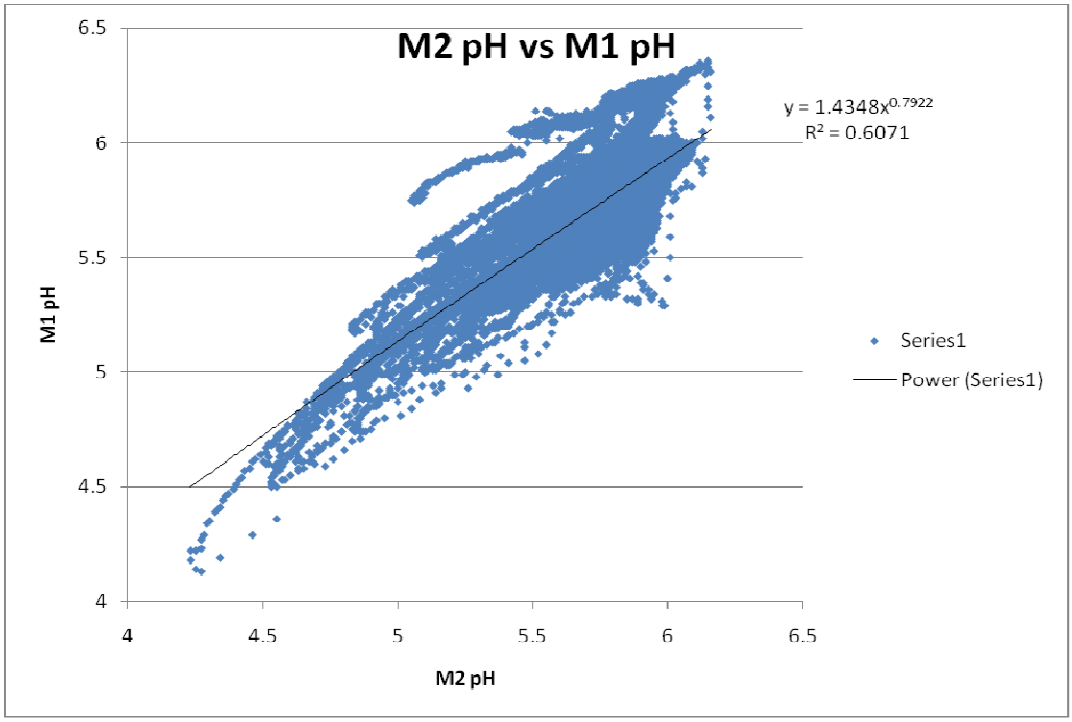

Figure 39. Ramsey Prong pH vs. Middle Prong pH regression

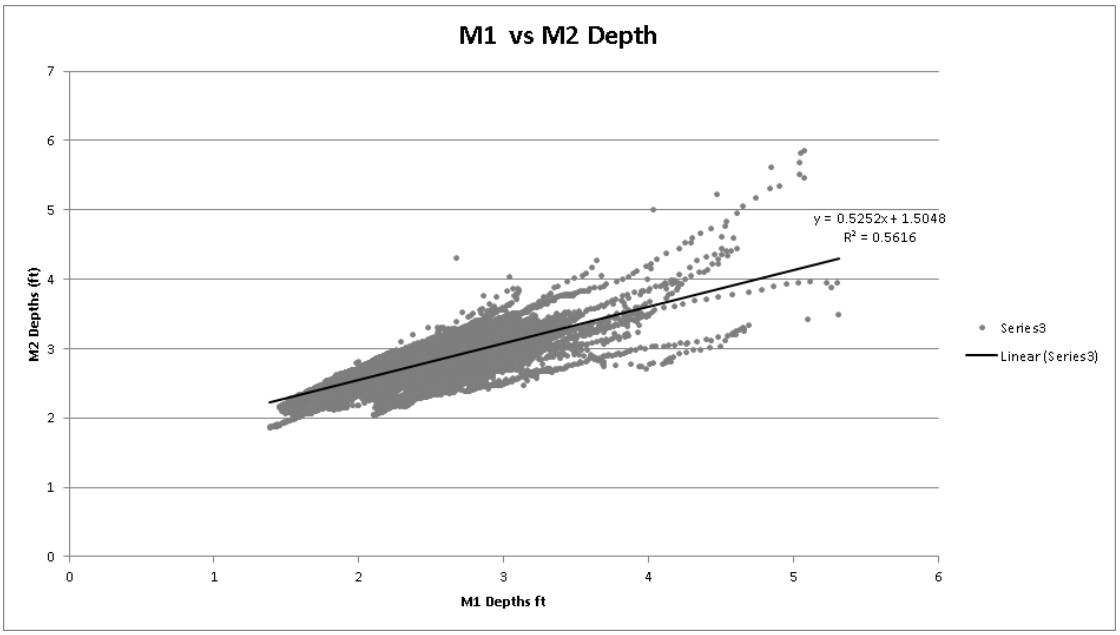

Figure 40. Middle Prong depth vs. Ramsey Prong depth regression

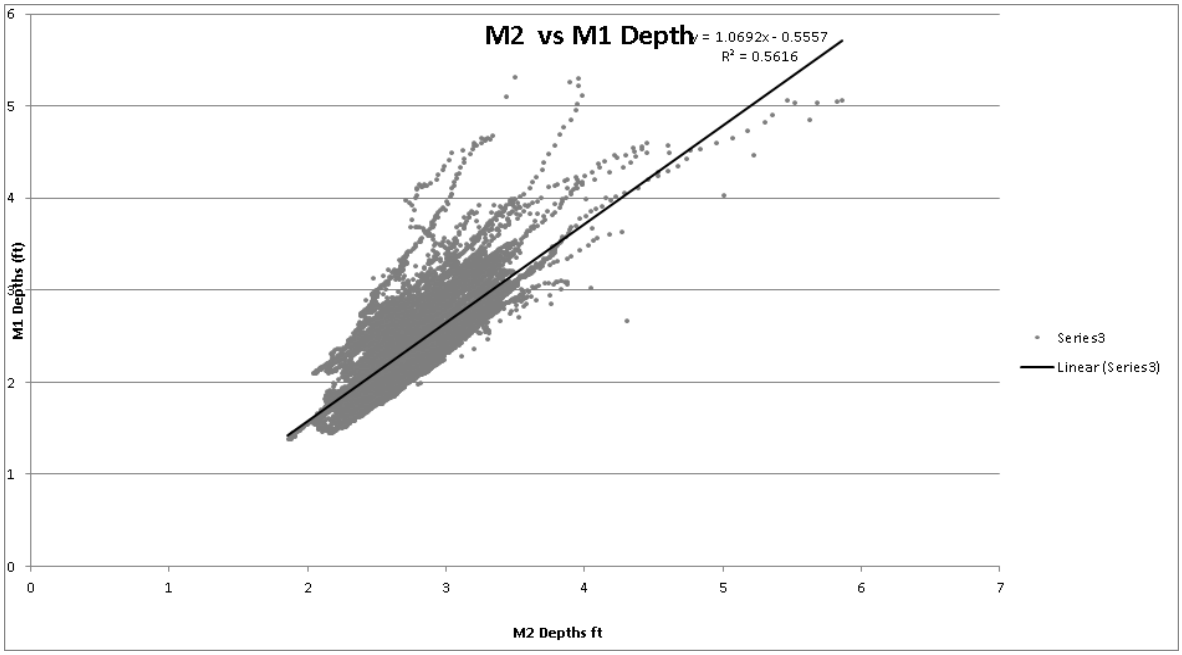

Figure 41. Ramsey Prong depth vs. Middle Prong depth regression

Appendix E: Chemographs for Sampled Storms Events

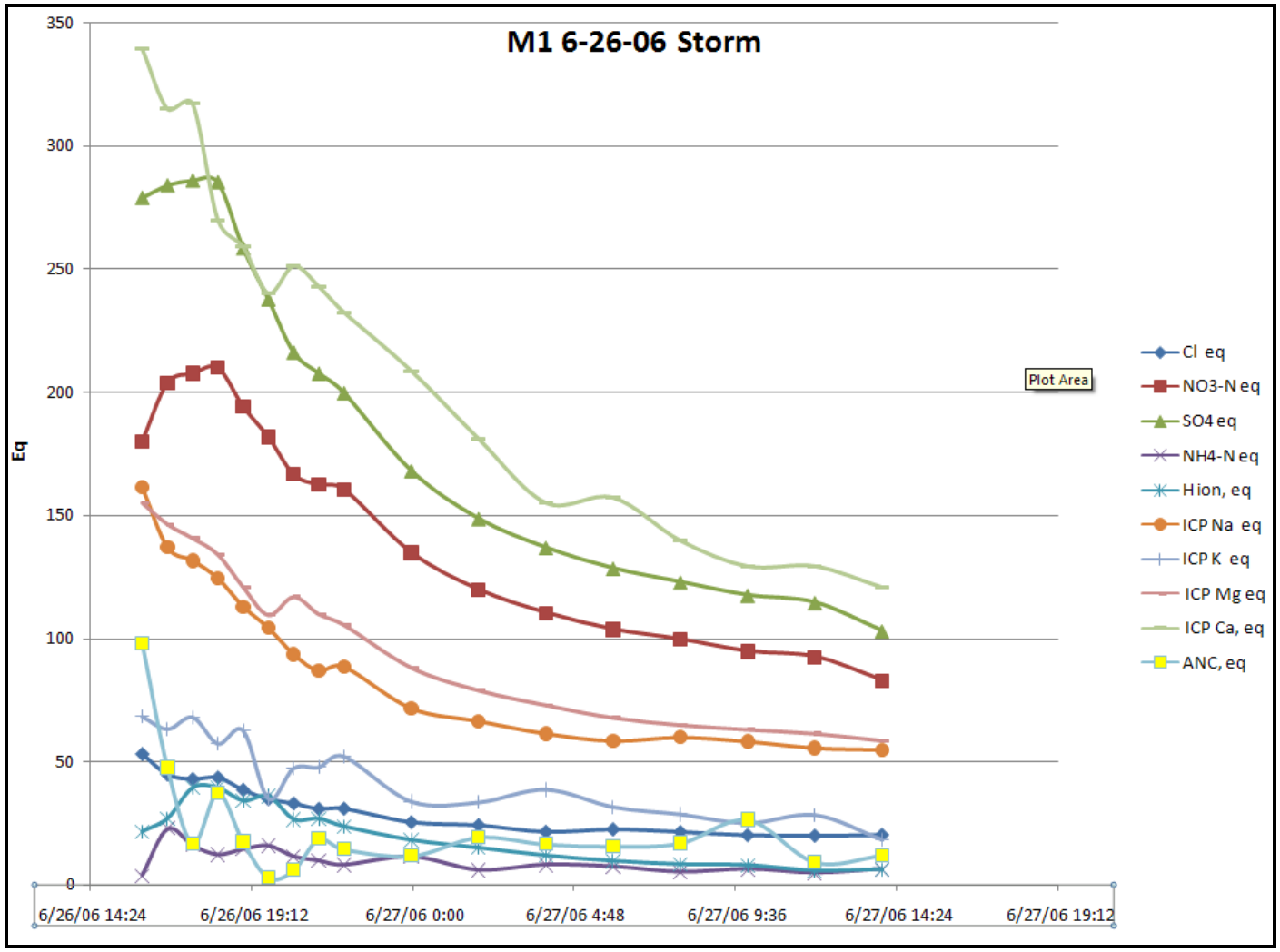

Figure 42. Middle Prong site chemograph for 6/26/06 storm

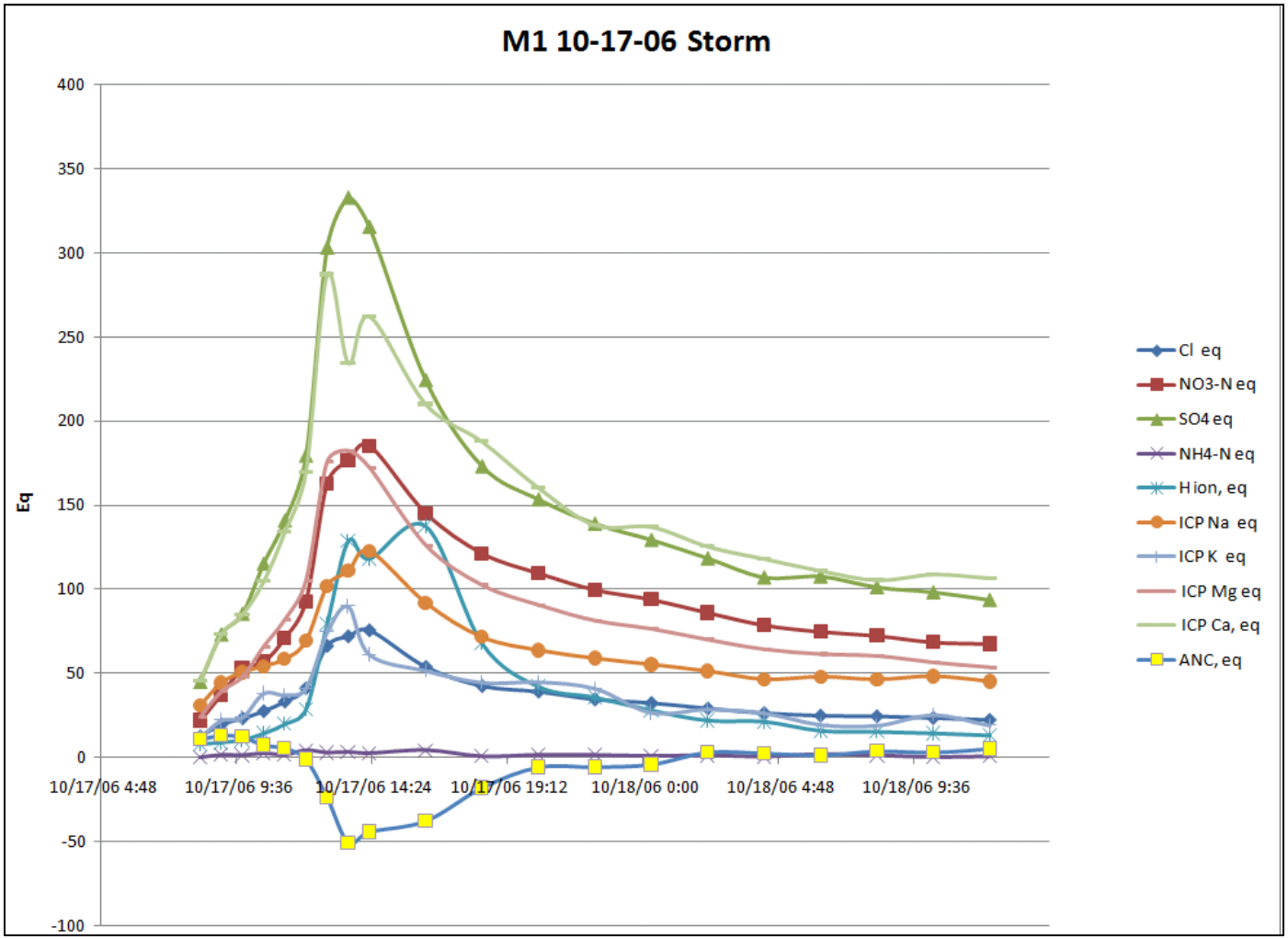

Figure 43. Middle Prong site chemograph for 10/17/06 storm

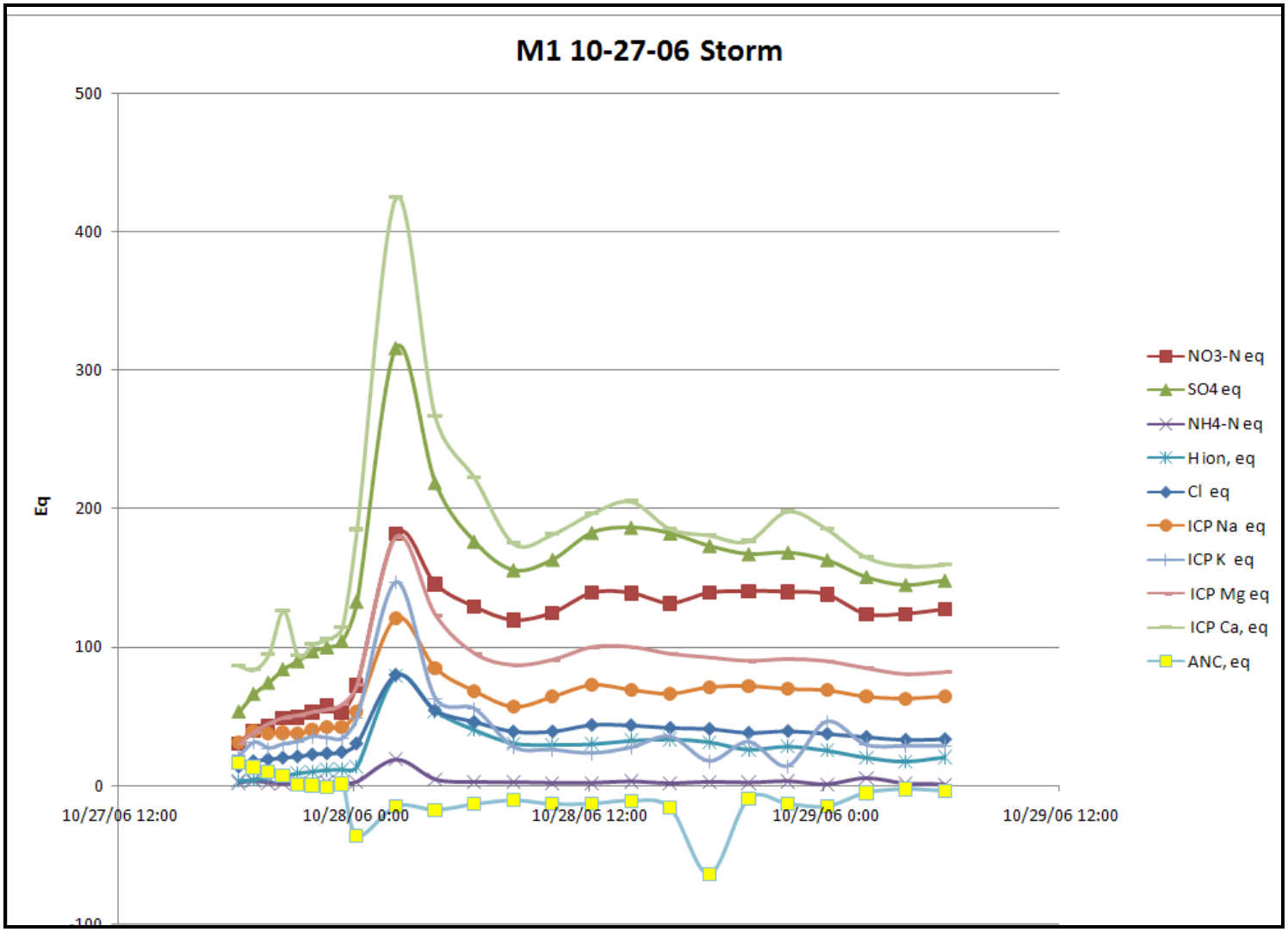

Figure 44. Middle Prong site chemograph for 10/27/06 storm

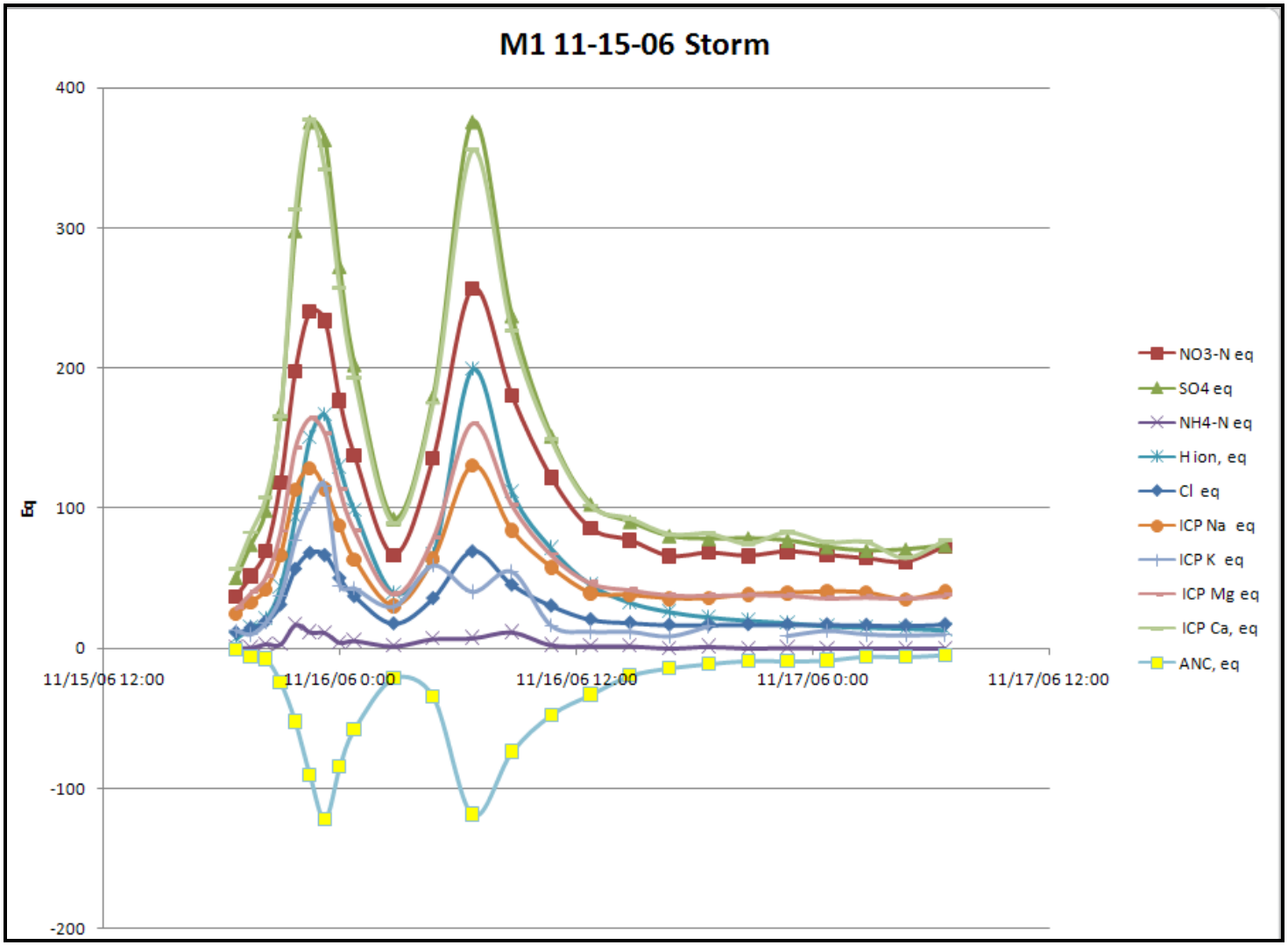

Figure 45. Middle Prong site chemograph for 11/15/06 storm

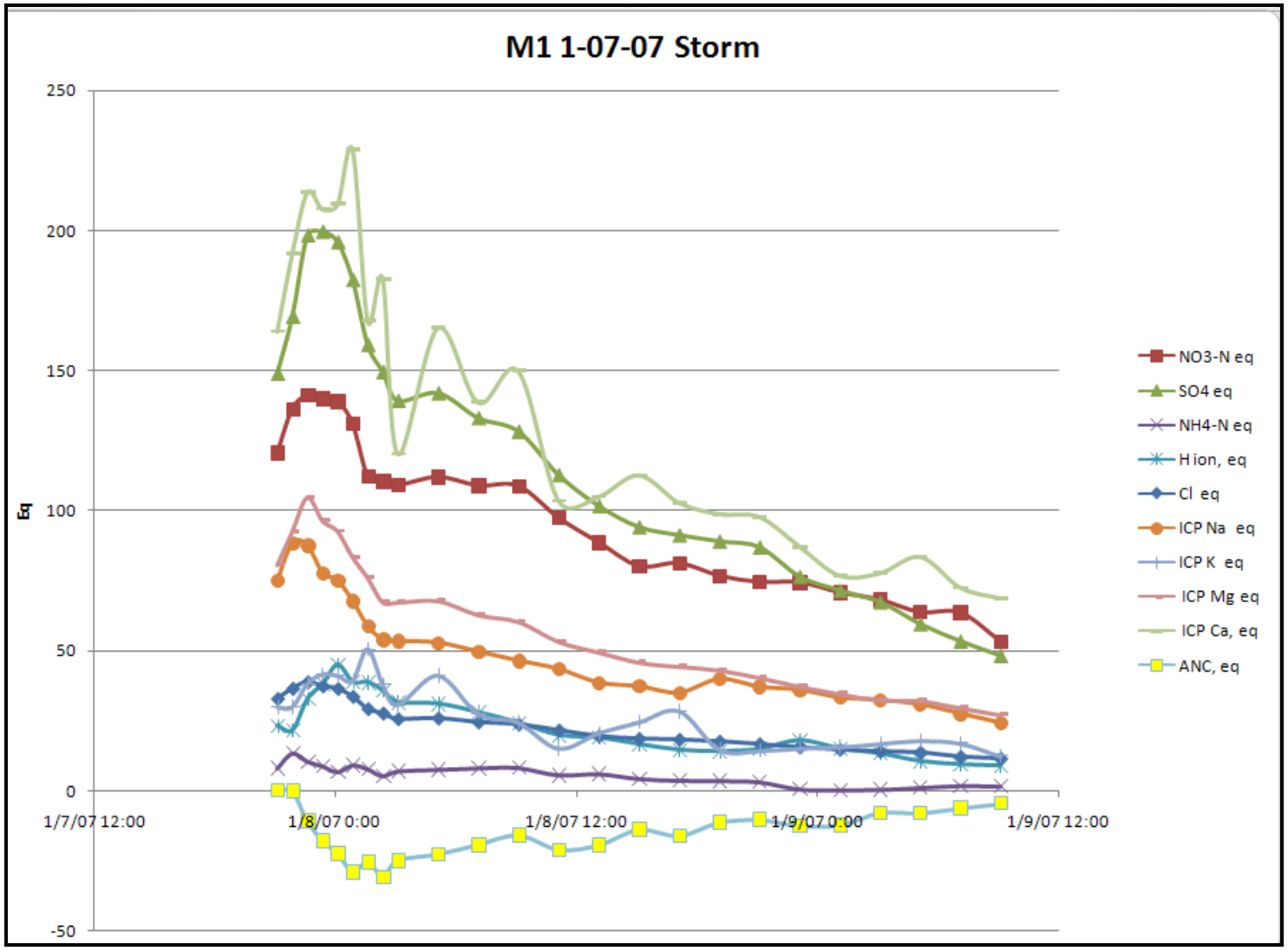

Figure 46. Middle Prong site chemograph for 1/7/07 storm

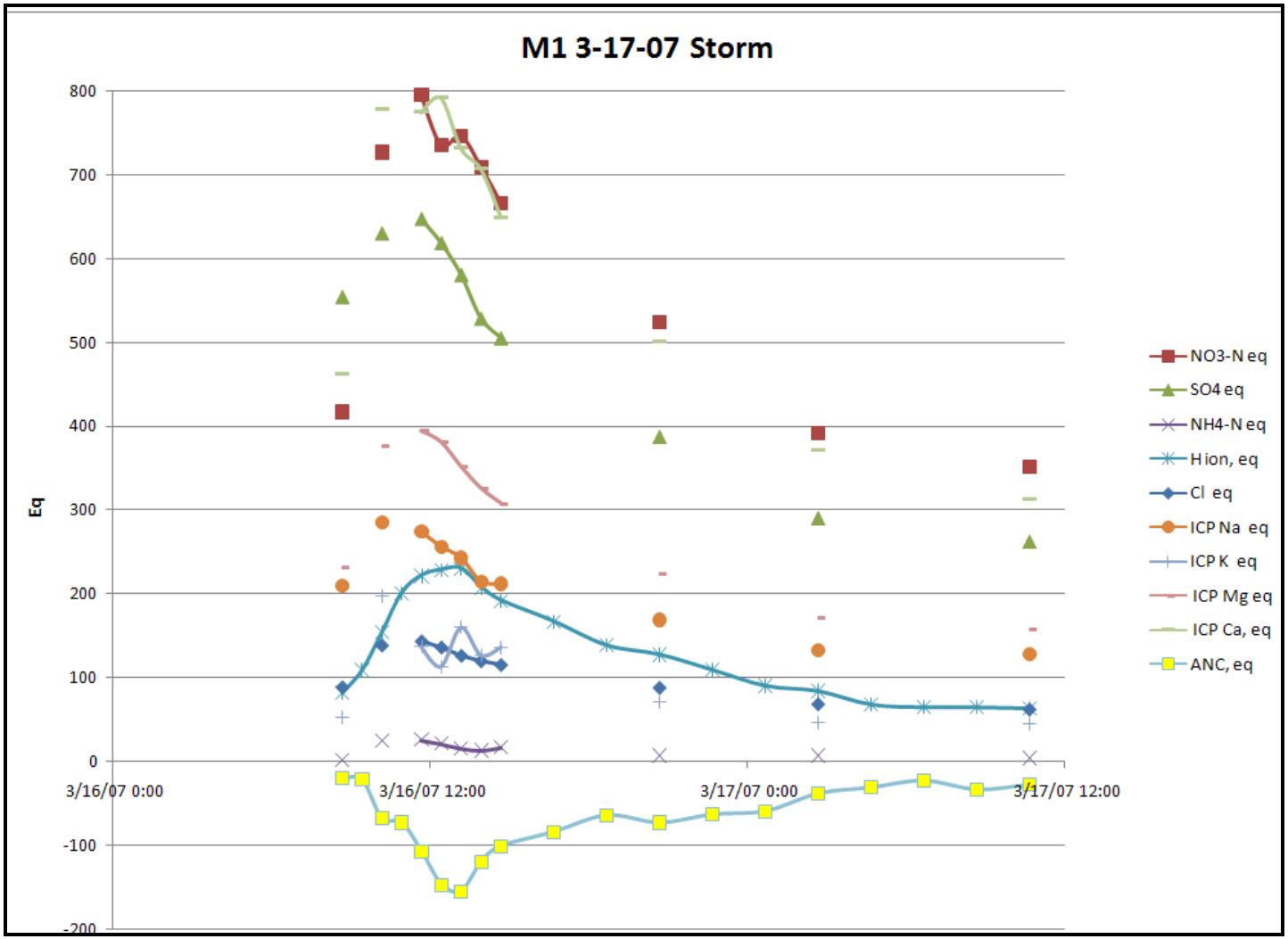

Figure 47. Middle Prong site chemograph for 3/17/07 storm

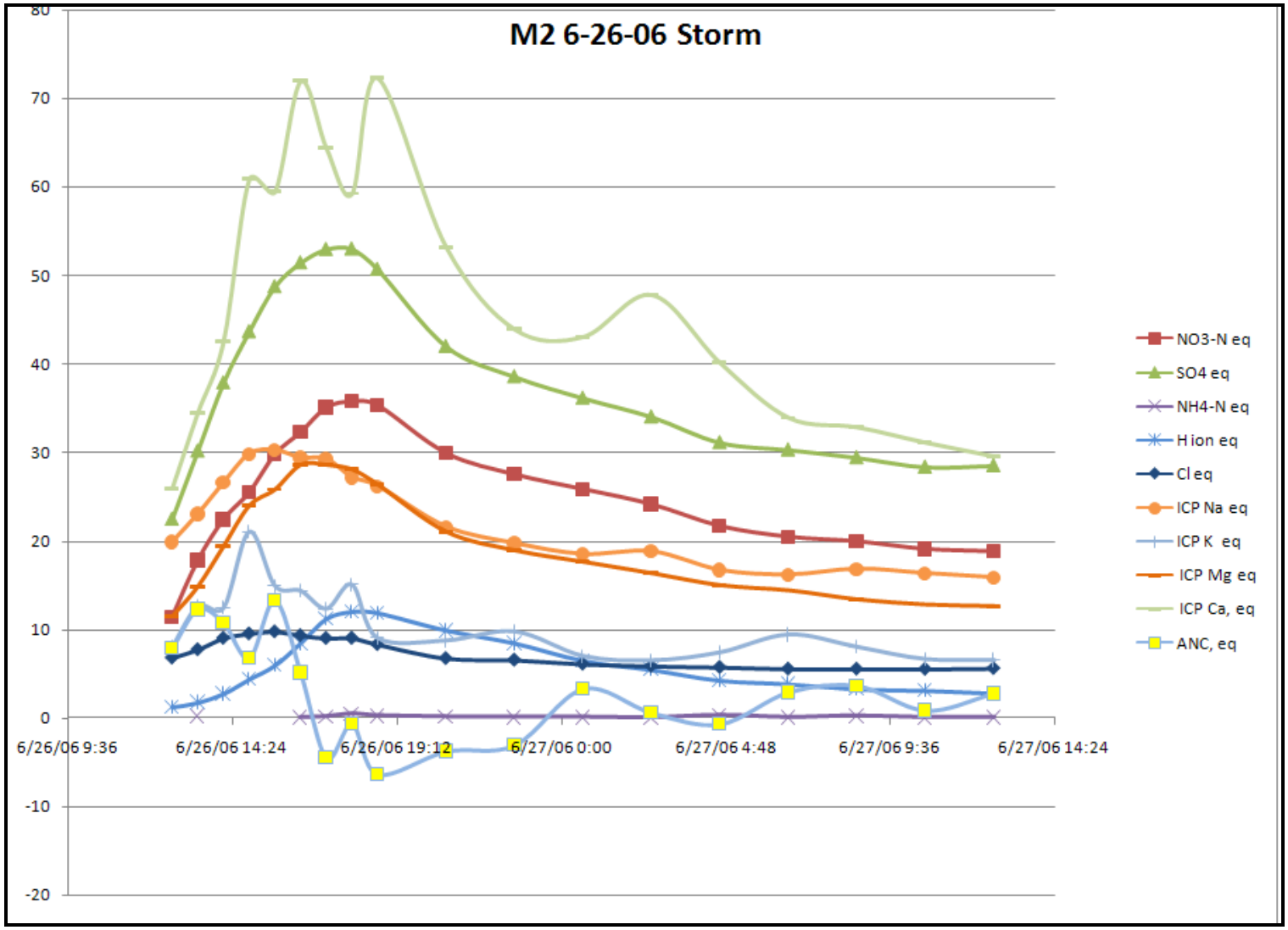

Figure 48. Ramsey Prong site chemograph for 6/26/06 storm

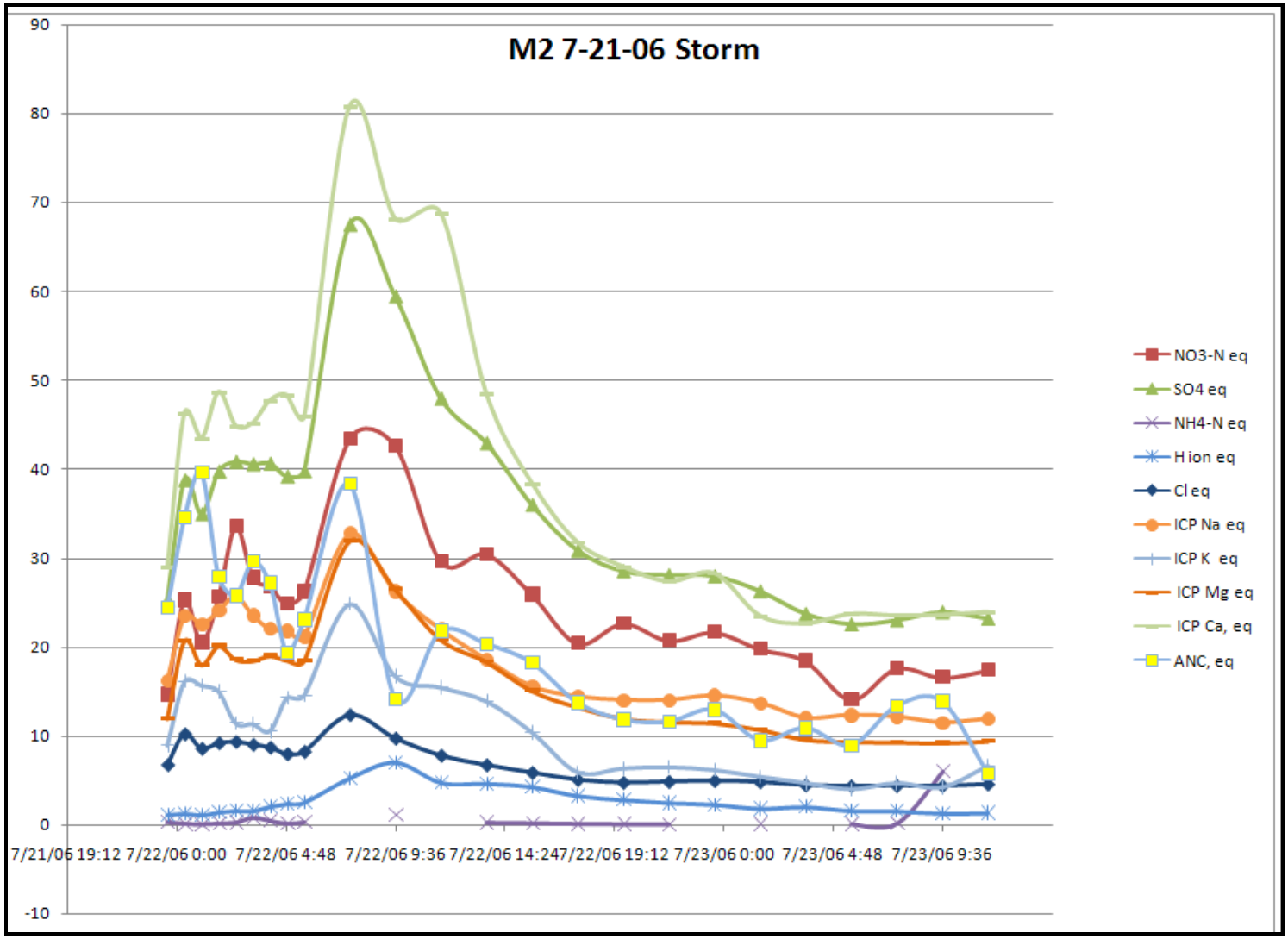

Figure 49. Ramsey Prong site chemograph for 7/21/06 storm

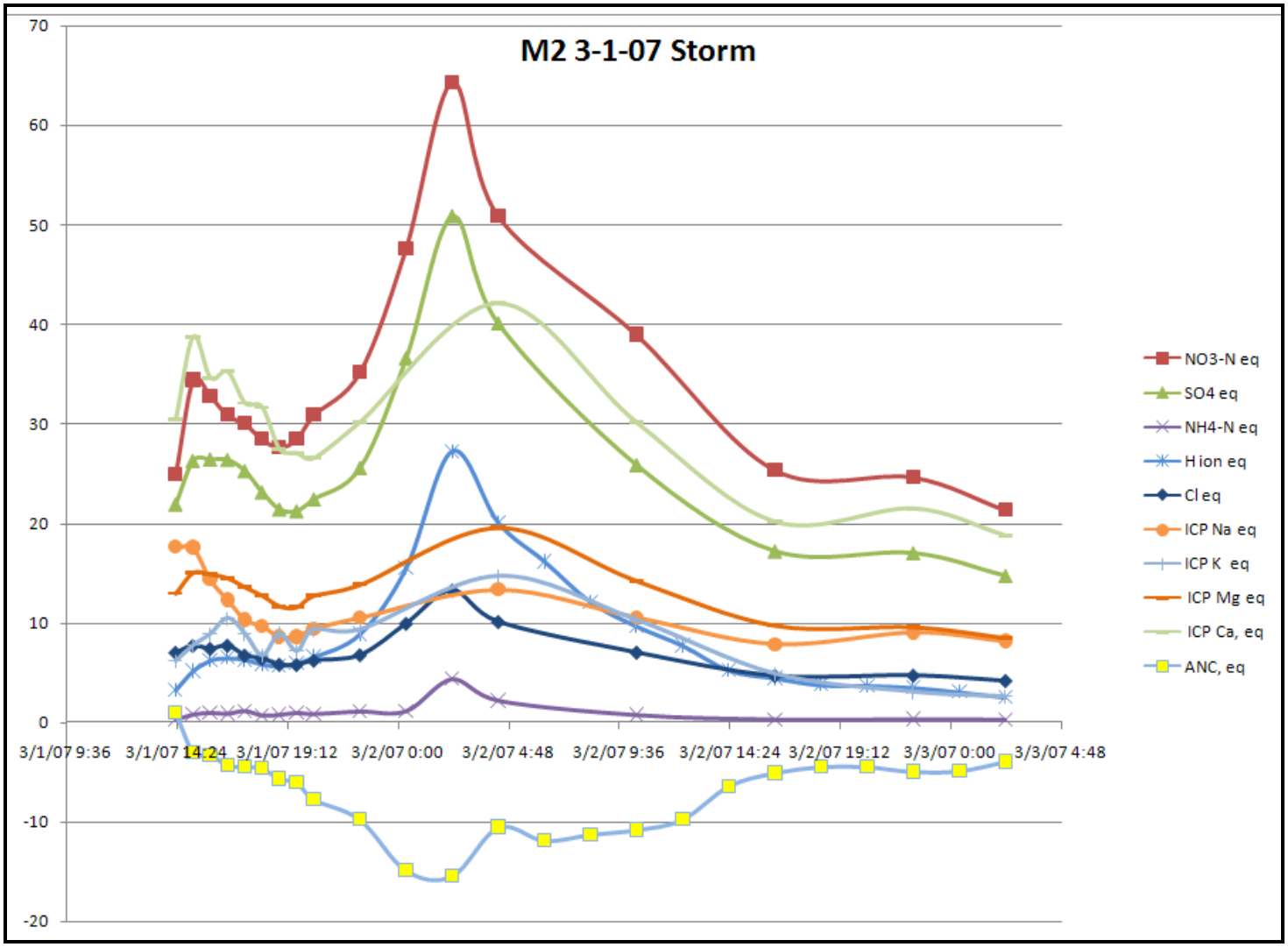

Figure 50. Ramsey Prong site chemograph for 3/1/07 storm

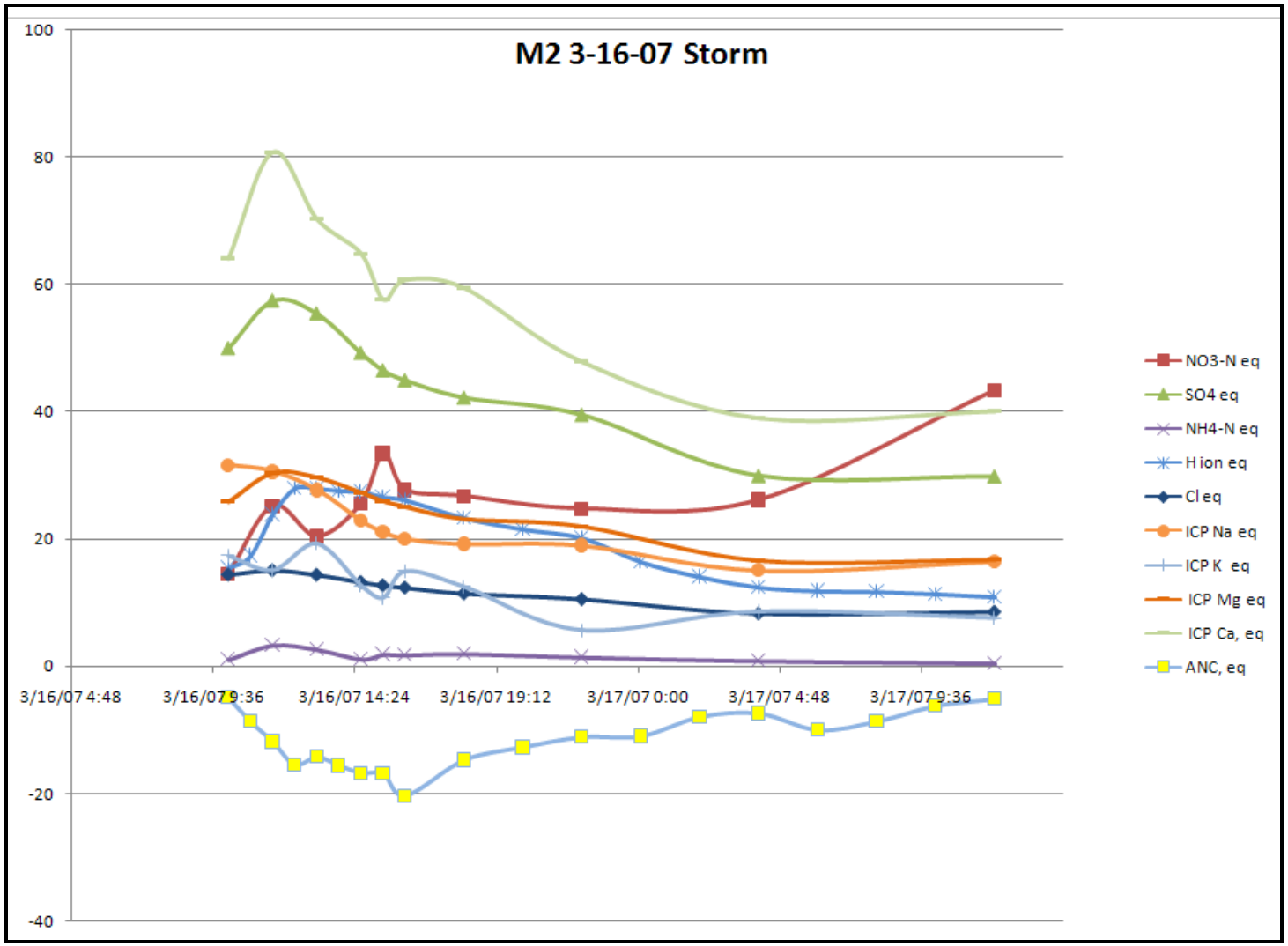

Figure 51. Ramsey Prong site chemograph for 3/16/07 storm

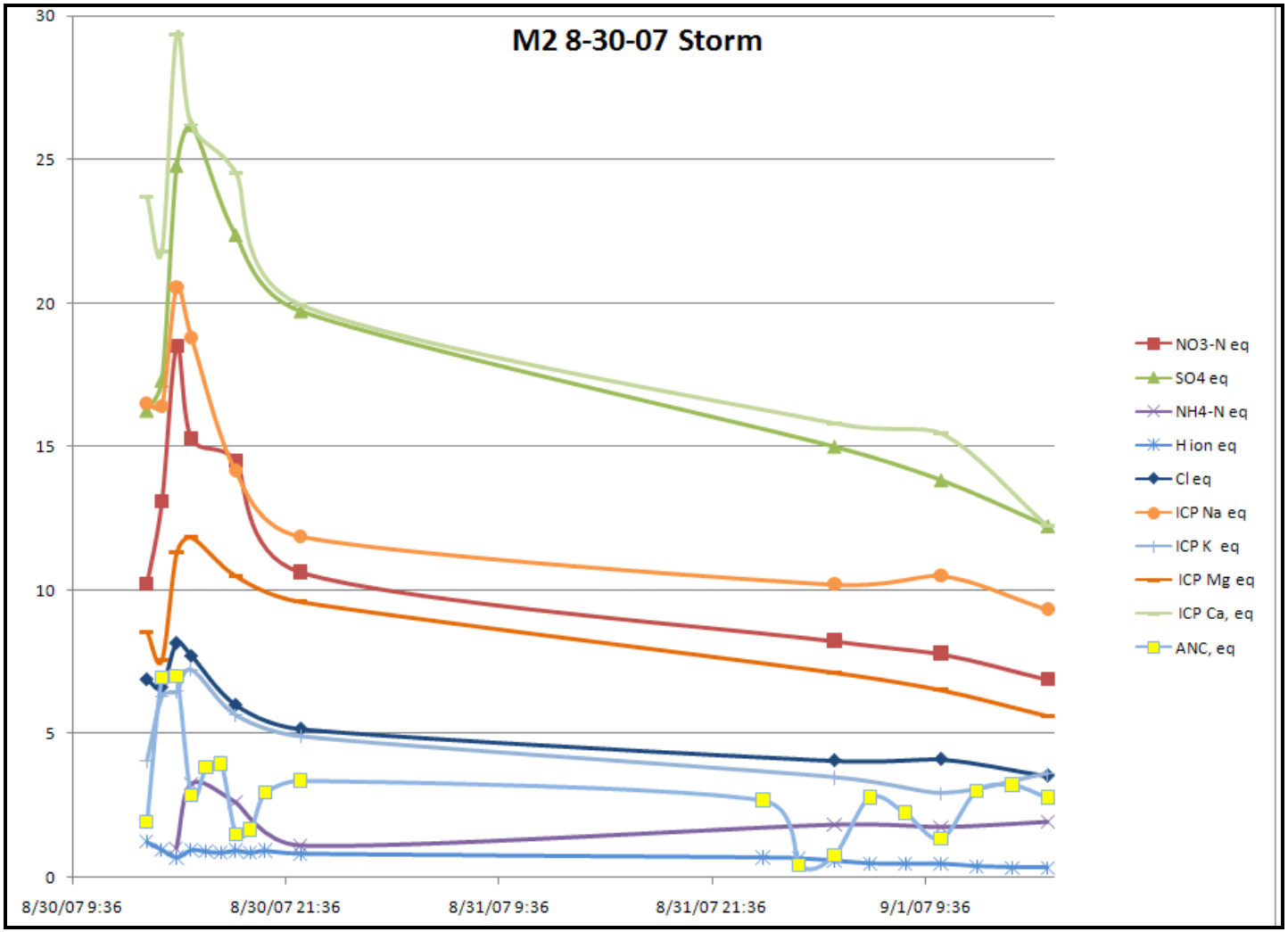

Figure 52. Ramsey Prong site chemograph for 8/30/07 storm

Appendix F: Photographs of Study Sites

Figure 53. Middle Prong sonde

Figure 54. In the middle of the Middle Prong reach viewing upstream

Figure 55. In the middle of the Middle Prong reach viewing downstream

Figure 56. General hydraulic complexity of the Middle Prong reach

Figure 57. Ramsey Prong sonde

Figure 58. Upstream boundary of Ramsey Prong reach

Figure 59. Viewing downstream from upper Ramsey Prong reach

Figure 60. Viewing upstream from middle of Ramsey Prong reach

Figure 61. Viewing upstream from Ramsey Prong reach outlet

VITA

Guy Thomas Zimmerman was born in Knoxville, Tennessee, at the University of Tennessee Hospital. After passing his formative years in Cookeville, Tennessee, he set out with his backpack to see America. He spent several years hiking the Appalachian, Colorado, and Pacific Crest Trails. The insights gained from his time in the backcountry led him back to the University of Tennessee and the Great Smoky Mountains for a formal education culminating in a Bachelor of Science in Civil Engineering with a Minor in Environmental Engineering and an informal education via whitewater kayaking culminating with an intimate knowledge of the hydrology and hydraulics of the mountain streams in southern Appalachia. He had the amazing opportunity to combine these knowledge centers during his graduate education through water quality research in the streams of the Great Smoky Mountains. Mr. Zimmerman is a consulting engineer in Knoxville, Tennessee. Mr. Zimmerman and wife, Sarah, have three children: Lily, Huck, and Roan.